MLC-based IMRT, but also for multi-purpose research [4–15]. However, it is necessary to verify the modeling accuracy of MLC on Monte Carlo simulation prior to use, because MLC has complicated structures, e.g., leaf tip, support rail groove, tongue-and-groove design, and a round leaf end. Therefore, MLC modeling is not easy. Thus, various tests after MLC modeling should be performed in the effort to ascertain whether the MLC structures are properly modeled in the Monte Carlo simulation. Some studies for modeling of MLC have been reported for Monte Carlo simulation EGS4 (electron gamma shower), which has been widely used in photon radiotherapy [16–19], but solid research for Monte Carlo simulation GEANT4 (GEometry ANd Tracking) [5] has not yet been reported. In this study, we proposed five tests for implementation of IMRT on Monte Carlo simulation, which focus on the leaf positions, inter-leaf/intra-leaf leakage, tongue-and-groove leakage, and a round leaf end on the GEANT4 simulation, based on a comparison with measurements.

Varian millennium 120-leaf collimators have some dosimetric characteristics [20–23], e.g., the Varian MLC has a role of effectively decreasing the leakage outside the field as tertiary collimators which are located beneath the collimator jaws. In addition, for effectively decreasing the leakage between the leaves, a tongue-and-groove design is implemented, and the round leaf end is designed so that the penumbra of the radiation field weakly depends on the positions of the leaves. These dosimetric characteristics need to be checked in the calculation in the Monte Carlo simulation for a dynamic MLC-based IMRT field.

2 Methods

2.1 GEANT4 and Validity for percentage depth-dose and off-central-axis ratio

The GEANT4 simulation (ver. 4.8.2.p01) [5] was performed by non-parallel computation on a 16-CPU Linux (RX-4000 Calm, Real Computing, Inc., Tokyo, Japan) in this study. The code GEANT4 simulation provides a number of user-selectable physics lists for the calculations [5]. In this study, "standard ElectroMagnetic (EM) physics" with a range cut value of 0.5 mm was used for calculation of the dose distribution. The standard EM physics is provided by the Electromagnetic standard physics working group established in the GEANT4 project. This code is prepared as GEANT4 sub-packages for simulation of electromagnetic interactions of charged particles, gammas, and optical photons. The validity range is from 1 keV to 10 PeV, but standard EM physics is optimal particularly in the range of high and medium energy applications.

For the parameters of the initial electron beam bombarding the tungsten target [24], i.e., the mean energy, the radial intensity distribution, and the spread of the mean energy, the same values were employed for 6 MV X-rays from the Varian clinac^{TM} (iX, Varian Medical Systems, Palo Alto, CA, USA) as those proposed by Sheikh-Bagheri and Rogers [25]. The Varian clinac^{TM} consists of a triode electron gun, an RF source (Klystron), wave guide, bending magnet, and gantry head. This system can produce a high-stability beam, enable us to perform the highly precise radiation therapy, such as dynamic arc conformal therapy and IMRT. To verify the validity of using these electron beam parameters for our Varian clinac^{TM}, we compared the calculated data with the measured data in depth-dose and lateral-dose profile for both small and large fields. In this measurement, a gantry/collimator angle of 0° and a dose rate of 300 MU/min for the Varian linac were set. The depth-dose for field sizes of 10 × 10 and 40 × 40 cm^2 was calculated by GEANT4 and obtained with ionization chambers (CC13, IBA dosimetry, Schwarzenbruck, Germany). The lateral-dose profile for field sizes of 10 × 10 and 35 × 35 cm^2 was calculated by GEANT4 and obtained with a diode detector (PFD, IBA dosimetry, Schwarzenbruck, Germany).

In addition, the photon energy distribution and lateral distribution of the photon fluence for a 35 × 35 cm^2 field by GENAT4 were compared with those by Monte Carlo simulation EGSnrc (ver. 4.2.3.2) with PCUT = 0.010 - MeV and ECUT = 0.700 MeV. To effectively reduce the calculation time [26], we used the phase-space binary file storing particle information (positions, kinds of particles, kinetic energy) above the field-defining collimator jaws in this study. The size of the phase-space binary file is 20 G bytes, which has approximately 1 × 10^{10} photons and electrons generated from the treatment head.

2.2 Varian millennium 120 leaf collimators

As shown in Fig. 1, almost full structures of Varian millennium 120 leaf collimators, i.e., leaf tip, support rail groove, tongue-and-groove design, and round leaf end design [16], etc. (except the screw-driving hole), were modeled on the Monte Carlo code GEANT4. In the GEANT4, the complexity of the structures of the Varian MLC can be checked by use of the graphical user interface (GUI) of OpenGL® (Khronos group Inc., Beaverton, OR, USA). An MLC density of 17.35 g/cm^3 was chosen in this study, which was proposed by Jang [17]. For verifying the MLC modeling on the GEANT4 simulation, five tests were performed: (I) MLC transmission, (II) MLC transmission profile (including intra-leaf and inter-leaf leakages), (III) tongue-and-groove leakage, (IV) composed field with different field sizes with use of MLC, and (V) a dynamic MLC-based IMRT field. For all tests, the

calculations were compared with the measurements of an ionization chamber or radiographic film. In the GEANT4 simulation, the two-dimensional dose distribution was calculated in each volume of $1 \times 1 \times 1$ mm^3 in the region of interest. The methods of the five tests are described in the following.

TEST (I): MLC transmission: A 0.6 cm^3 Farmer chamber (30013, PTW, Freiburg, Germany) was placed at a depth of 10 cm in water with a source-to-chamber distance of 100 cm. The MLC transmission (all leaf positions of 7 cm perpendicular to a beam central axis at the isocenter with the jaws open to a 10×10 cm^2 field) was measured with the ionization chamber, and was also calculated with the GEANT4 simulation. The measured leakage included both intra- and inter-leaf leakage, because a 0.6 cm^3 Farmer chamber with a length of 22 mm can cover approximately four MLCs (leaf width of 5 mm).

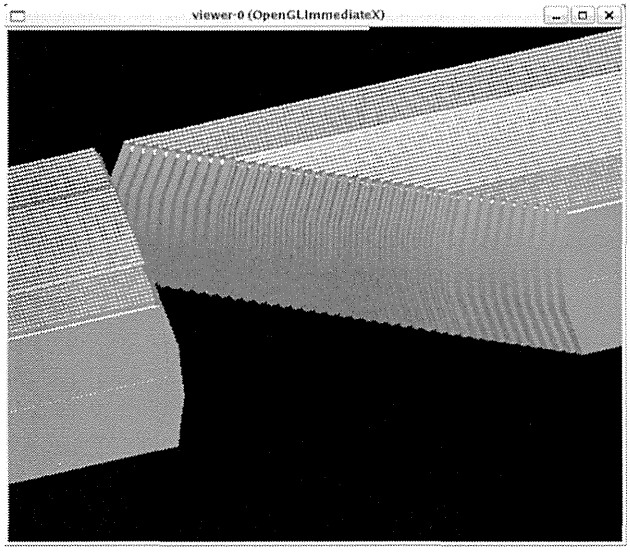

Fig. 1 Graphics of Varian MLC on the GEAN4 simulation. The Varian MLC consists of 80 inner leaves (0.5 cm width at isocenter) and 40 outer leaves (1.0 cm width at isocenter)

TEST (II): MLC transmission profile (including intra- and inter-leaf leakage): The irradiation condition was the same as that of test (I). For obtaining the leaf leakage profile in the longitudinal direction of the closed field by the MLC, a radiographic film (X-OMAT, Eastman-Kodak Company, Rochester, NY, USA) was placed at a depth of 10 cm in a water-equivalent phantom (tough water phantom, Kyoto Kagaku co., Kyoto, Japan) with a source-to-film distance of 100 cm. The resolution of the scanner (ES-8500, SEIKO EPSON Corporation, Nagano, Japan) was 150 dpi (approximately 0.2 mm/pixel). The optical density was converted to absorbed dose with use of the calibration table in the film analysis software (DD-system, R-TECH Company, Tokyo, Japan).

TEST (III): Tongue-and-groove leakage: The irradiation field was composed of two fields for obtaining the tongue-and-groove leakage by radiographic film. In one of them, the even leaves are open and the odd leaves are closed (Fig. 2a). In the other, the even leaves are closed and the odd leaves are open (Fig. 2b). The radiographic film was irradiated with the two sub-fields with the same monitor units.

TEST (IV): Composed field with different field sizes: A simple field was composed of three fields with three different field sizes of the MLC, i.e., field widths of 1, 5, and 10 cm by the MLC with fixed jaws of 20×20 cm.

TEST (V): Dynamic MLC-based IMRT field: Radiographic film was placed at a depth of 5 cm in a water-equivalent phantom (tough water phantom) with a source-to-surface distance of 95 cm. The IMRT field used as clinical treatment for head and neck cancer was calculated on the GEANT4 simulation. In this study, the dose distribution of the IMRT field with dynamic MLC was calculated by integration of the dose distribution of each control

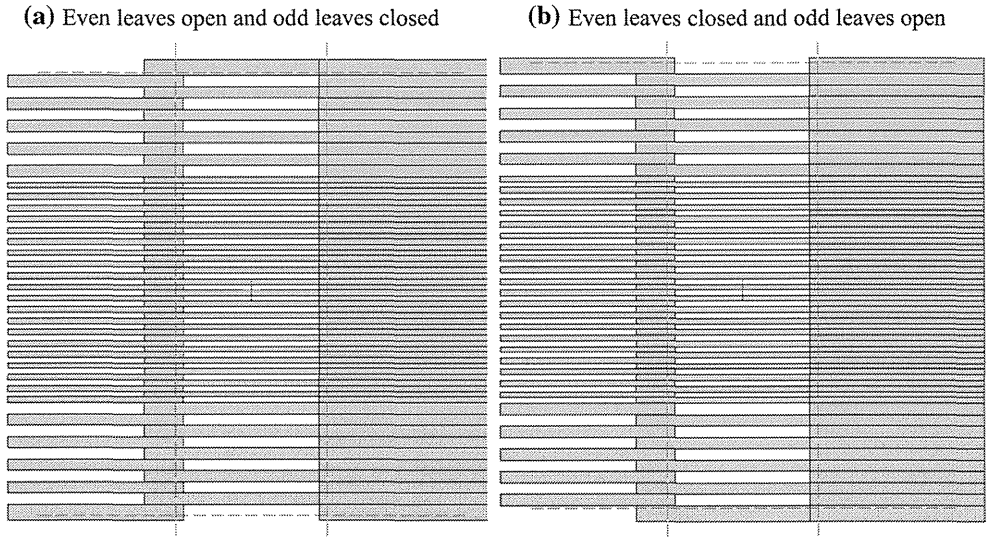

Fig. 2 Obtaining tongue-and-groove leakage by use of the radiographic film, which was irradiated with the two fields (**a**, **b**) with the same monitor units

point of MLC movement without smoothing of MLC positions between control points for easily calculation. Since early times, an effort has been made quantitatively to evaluate the two-dimensional distributions such as the film dose, and various approaches have been addressed [27–29]. The gamma evaluation method has recently been generalized for IMRT verification, which was proposed by Low [30, 31]. In the (IV) and (V) tests, the dose distributions calculated with the GEANT4 simulation were evaluated by the gamma evaluation method with the criterion of 3 % of local dose difference and 3 mm distance to agreement (DTA) (reference = film, evaluation = GEANT4) [30]. In addition, interpolation between dose pixels (pitch of 1 mm) was done, obtaining the minimum gamma value at each

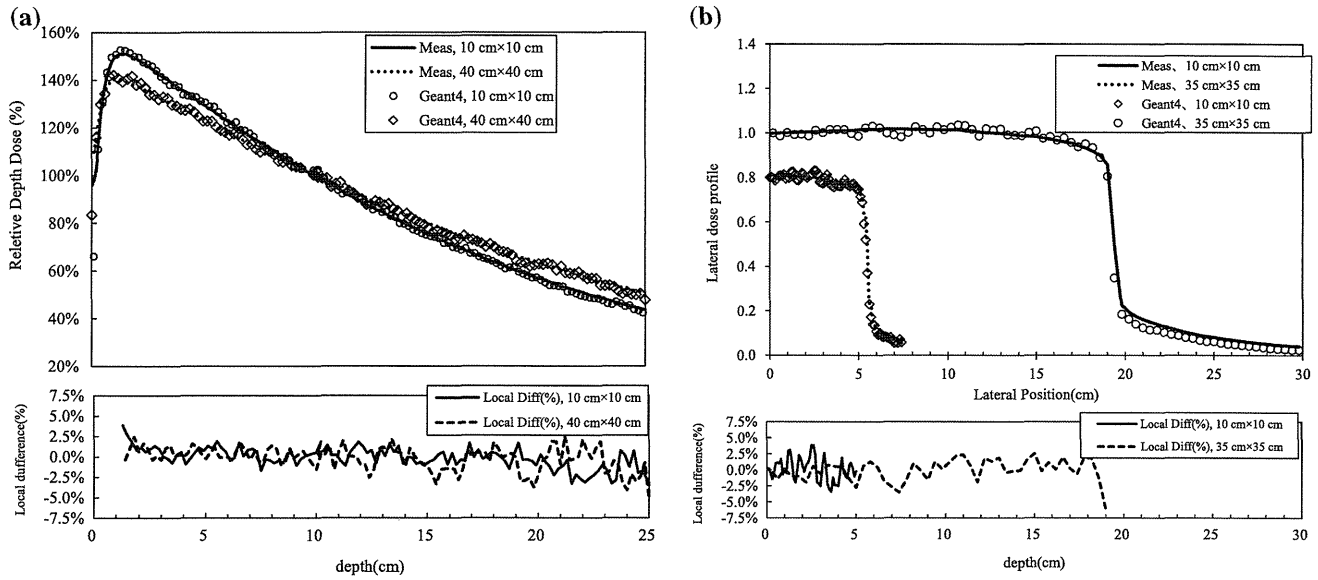

Fig. 3 **a** Comparison of measured and calculated depth-dose curves with the 10 × 10 and 40 × 40 cm^2 fields for 6 MV X-rays. The depth-dose curves are measured with ionization chambers (CC13). All data were normalized to the value at 10 cm depth. **b** Comparison of measured and calculated dose profiles at 10 cm depth with the 10 × 10 and 35 × 35 cm^2 field for the 6 MV X-rays. The center value of dose profile for 10 × 10 cm^2 was normalized at 0.8 for ease of reading the figure. The measurements were made with a diode detector (PFD)

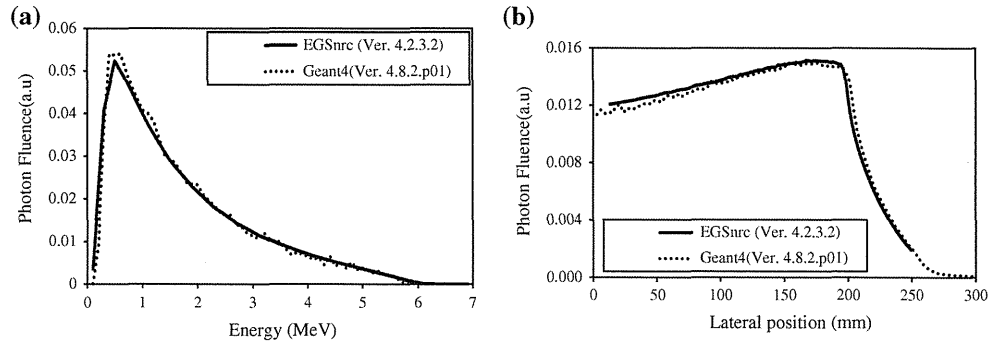

Fig. 4 Photon energy distribution at a distance of 100 cm from the target in air, and lateral distribution of photon fluence in air by GEANT4 and EGSnrc

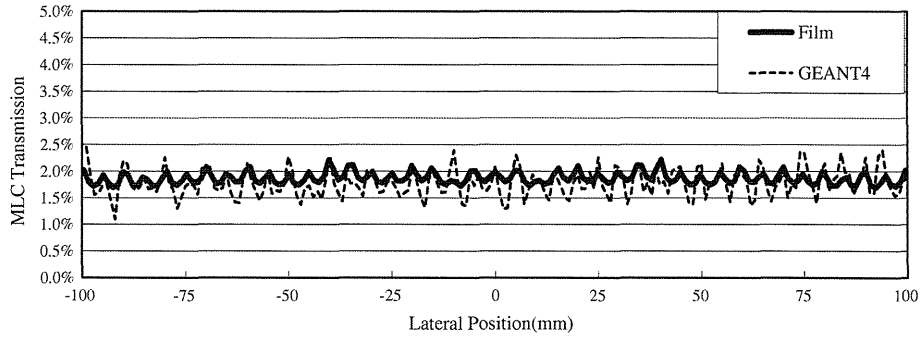

Fig. 5 The MLC transmission profile in the longitudinal direction of the closed field by the Varian MLC was calculated with GEANT4 simulation and measured with radiographic film

point of Ref. [32]. A threshold of 10 % of the maximum dose was used in this study, because the gamma value has a higher sensitivity to lower dose [33].

3 Results and discussion

3.1 Validity for percentage depth-dose and off-central-axis ratio

Figure 3a represents the depth-dose for field sizes of 10 × 10 and 40 × 40 cm^2 by the GEANT4 simulation and the measurements, respectively. Both dose curves were normalized at a depth of 10 cm. As shown in the figure, the dose distributions by the GEANT4 simulation agreed with the measured ones with a 1σ (one standard deviation) level (one standard deviation) of local differences of 1.4 and 1.4 %, for field sizes of 10 × 10 and 40 × 40 cm^2, respectively, in the region past the depth of the maximum. Figure 3b represents the lateral-dose profile for field sizes of 10 × 10 and 35 × 35 cm^2 by the GEANT4 simulation and the measurements, respectively. The center value of the lateral-dose profile for 10 × 10 cm^2 was normalized at 0.8 for ease of reading the figure. The dose distributions by the GEANT4 simulation agreed with the measured ones with a 1σ level of local difference of 1.9 and 1.5 %, for field sizes of 10 × 10 and 35 × 35 cm^2, respectively, in the region of the radiation field.

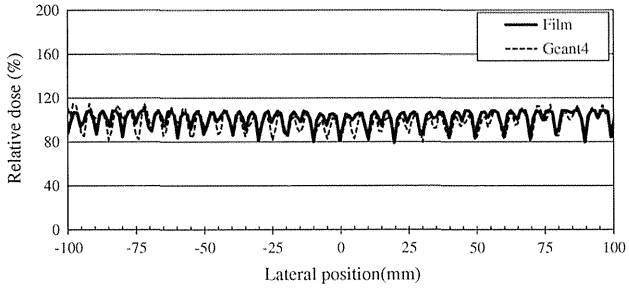

Fig. 6 Dose profile with the tongue-and-groove effect

Figure 4 depicts photon energy distribution at a distance of 100 cm from the target in air and the lateral distribution of photon fluence in air by GEANT4 and EGSnrc. It can be seen that GEANT4 can produce almost the similar distributions of photon energy and fluence, which proved that shape and materials of the target and flatness filter were properly modeling.

3.2 TEST (I) and (II) MLC transmission and profile

TEST (I): The MLC transmissions by calculation and measurement were 1.76 ± 0.01 and 1.87 ± 0.01 %,

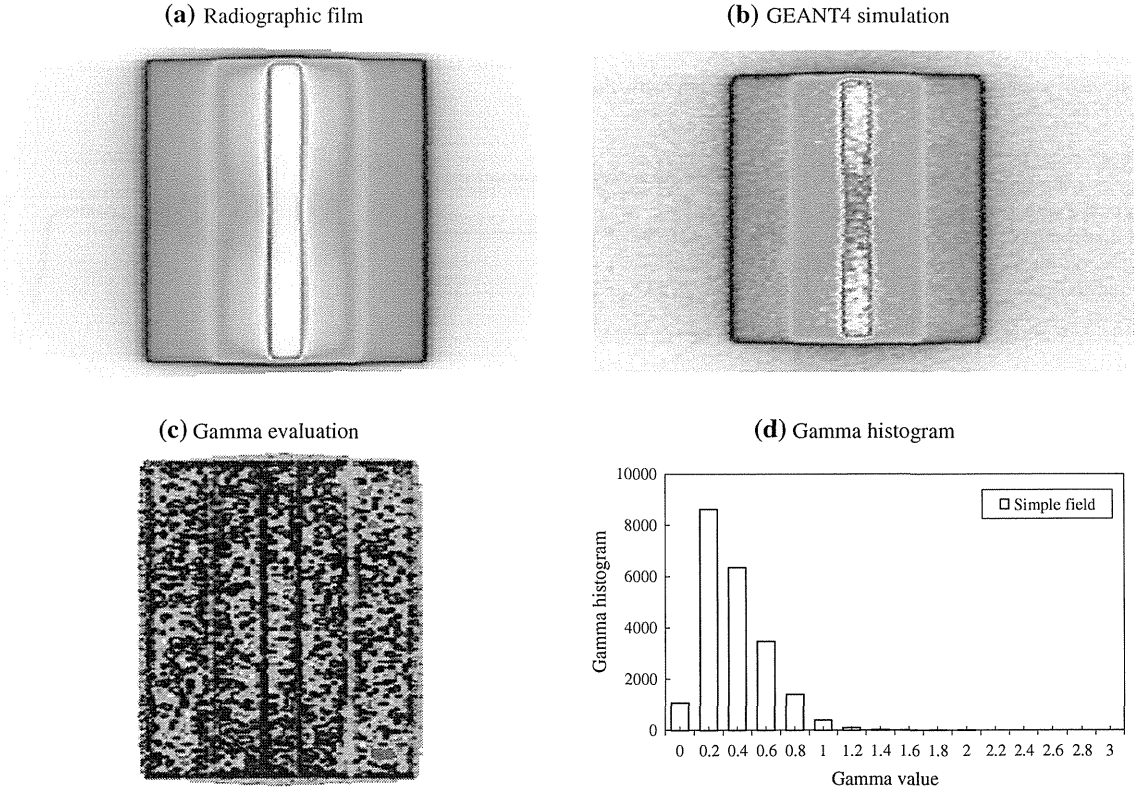

Fig. 7 Gamma evaluation of the simple field by the static MLC. **a** Radiographic film, **b** GEANT4 simulation, **c** gamma evaluation, and **d** gamma histogram. The criterion of 3 % of local dose difference and 3 mm DTA with the threshold of 10 % of the maximum dose was used in this study

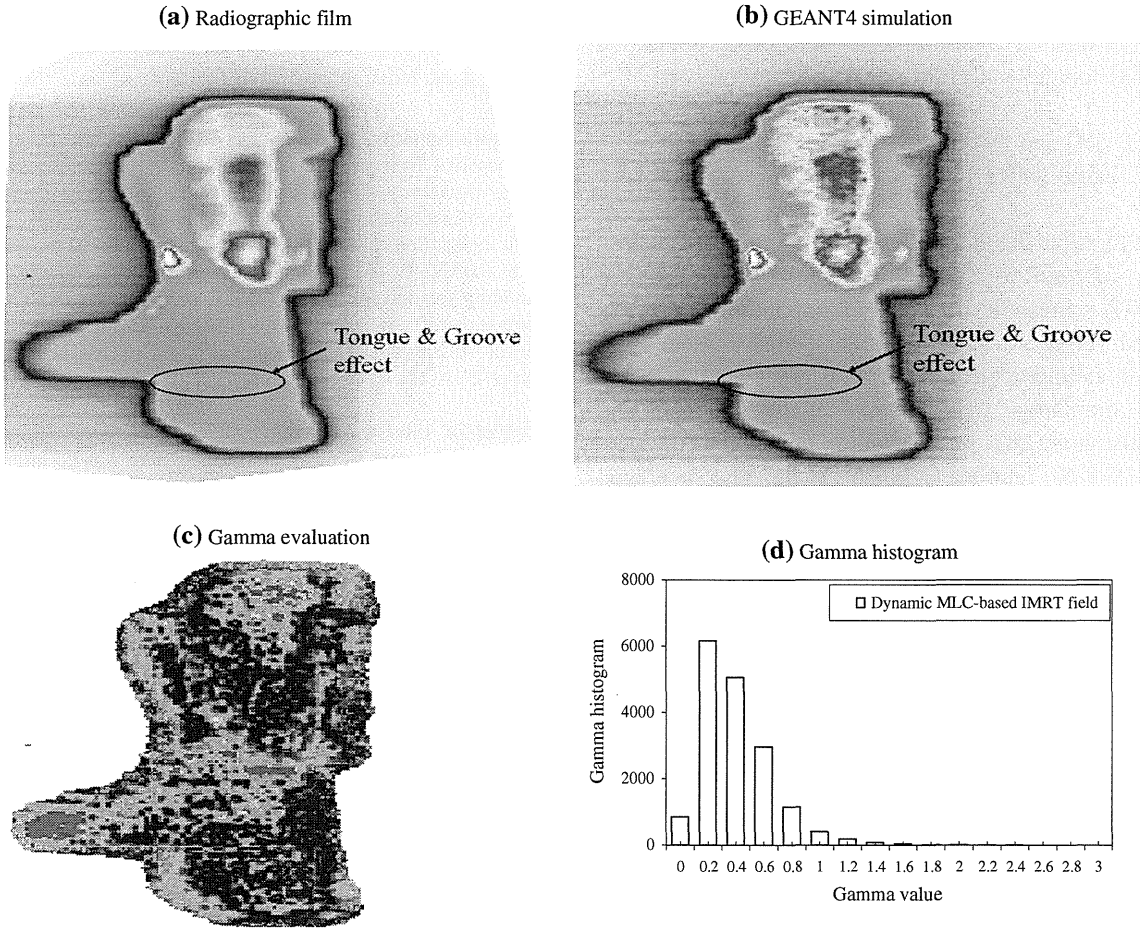

Fig. 8 Gamma evaluation for the dynamic MLC-based IMRT field (head & neck). **a** Radiographic film, **b** GEANT4 simulation, **c** gamma evaluation, and **d** gamma histogram. The criterion of 3 % of local dose difference and 3 mm DTA with the threshold of 10 % of the maximum dose was used in this study

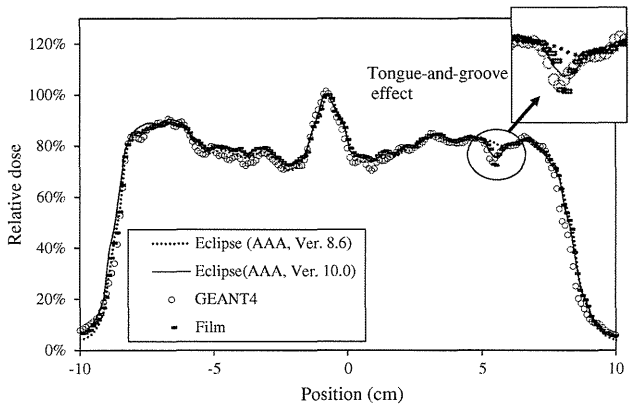

Fig. 9 Comparison of dose profiles in the longitudinal direction of the dynamic MLC-based IMRT field (Fig. 8) for radiographic film, the GEANT4 simulation, and the commercial TPS (Eclipse)

respectively. The calculation was a little lower than the measurements because the screw-driving hole is not considered on the GEANT4 simulation.

TEST (II): Figure 5 shows the MLC transmission dose profile in the longitudinal direction of the closed field by the MLC (all leaf positions of 7 cm at the isocenter with the jaws open to a 10 × 10 cm^2 field), which was calculated with the GEANT4 simulation and measured with radiographic film. The data acquired were normalized to agree with the measured MLC transmission. As can be seen in the figure, troughs and peaks exist at the same positions for both profiles, which correspond to the intra- and inter-leaf leakage, respectively. The GEANT4 simulation precisely calculates both leaf leakages.

3.3 TEST (III) Tongue-and-groove effect

Figure 6 shows the dose profile with the tongue-and-groove effect in the longitudinal direction of the two sub-fields (Fig. 2), which were calculated with the GEAN4 simulation and measured with radiographic film. The data acquired were normalized to be unity at the isocenter. Approximately 15–20 % decreases in the

region of the tongue-and-groove design for both the calculations and the measurements were observed, which means that tongue-and-groove leakage was present.

3.4 TEST (IV) and (V) Simple field and dynamic MLC-based IMRT field

TEST (IV): For the simple field, a gamma evaluation with the criterion of 3 % of local dose difference and 3 mm DTA (threshold of 10 % of maximum dose) was performed. Figure 7 shows the dose distribution measured with radiographic film (a) and calculated with the GEAN4 simulation (b), gamma evaluation (c), and gamma histogram (d). In the gamma evaluation, the pass rate of 98.5 % (gamma value >1) and the averaged gamma value of 0.35 (0–2.09) were given. Furthermore, good results in the boundaries of different field sizes of MLC (field widths of 1, 5, 10 cm) were also observed.

TEST (V): For the dynamic MLC-based IMRT field (head & neck), the gamma evaluation with the same criterion was also performed. Figure 8 shows the dose distributions measured with the radiographic film (a) and calculated with the GEAN4 simulation (b), gamma evaluation (c), and gamma histogram (d). In the gamma evaluation, a pass rate of 97.0 % (pass rate: percentage of gamma value ≤ 1) and an averaged gamma value of 0.38 (0–2.42) were given. There is a low-dose region by the tongue-and-groove effect (see Fig. 9) [23], which is indicated by arrows in Fig. 8a, b. Therefore, it can be proved that the tongue-and-groove design was modeled precisely in the GEANT4 simulation. It was not long ago that the complex structure of the MLC such as the round leaf end and tongue-and-groove design could not be modeled for dose calculation in the commercial TPS. A current TPS has been developed with a sophisticated model of MLC for dose calculation. Figure 9 shows the dose profiles in the longitudinal direction of the IMRT field (Fig. 8) for the commercial TPS (Eclipse ver. 8.6 and ver. 10.0, Varian Medical Systems Co., Palo Alto, CA), the radiographic film, and the GEANT4 simulation. The ver. 10.0 analytical anisotropic algorithm (AAA) [34, 35] can calculate the tongue-and-groove leakages, but ver. 8.6 AAA cannot do that, as seen in the figure. As indicated by an arrow in the figure, there is no low-dose region by the tongue-and-groove effect in ver. 8.6 AAA, but it can be observed in radiographic film, ver. 10.0 AAA, and the GEANT4 simulation.

4 Conclusions

In this study, the Varian millennium 120 leaf collimators were modeled on the Monte Carlo code GEANT4. To verify the MLC modeling, we performed five tests based on a comparison with measurements. The results of all tests were good, and the Monte Carlo code GEANT4 was proved to be a useful tool for calculating dose distributions of dynamic MLC-based IMRT.

Acknowledgments The authors wish to thank Dr. Tsukasa Aso of the Nagaoka University of Technology, Dr. Makoto Sakama of the Nihon University, Dr. Yuki Kase of the Shizuoka Cancer Center Research Institute, and Hideyuki Mizuno of the National Institute of Radiological Sciences for useful technical support of the Monte Carlo code GEANT4. The authors appreciate Varian Medical Systems providing the specifications of MLC only for researcher for Monte Carlo study of Varian linac. This study was partially supported by the Cancer Research and Development Fund of the National Cancer Center 23-A-13.

Conflict of interest There is no ethical problem or conflict of interest with regard to this manuscript. There was no human subject and no animal experiment in this study.

References

1. Wang L, Chui CS, Lovelock M. A patient-specific Monte Caro dose calculation method for photon beams. Med Phys. 1998;25:867–78.
2. Ma C-M, Mok E, Kapur A, Pawlicki T, Findley D, Brain S, Forster K, Boyer AL. Clinical implementation of a Monte Carlo treatment planning system. Med Phys. 1999;26:2133–43.
3. Ma C-M, Boyer AL. Monte Carlo verification of IMRT dose distributions from a commercial treatment planning optimization system. Phys Med Biol. 2000;45:2483–95.
4. Rogers DWO, Faddegon BA, Ding GX, Ma C-M, We J. BEAM: a Monte Carlo code to simulate radiotherapy treatment units. Med Phys. 1995;22:503–24.
5. Agostinelli S, et al. GEANT4—a simulation toolkit. Nucl Instrum Methods Phys Res. 2003;A506:250–303.
6. Chetty IJ, Curran B, Cygler JE, DeMarco JJ, Ezzell G, Faddegon BA, Kawrakow I, Keall PJ, Liu H, Ma C-M, Rogers DWO, Seuntjens J, Sheikh-Bagheri D, Sievers JV. Report of the AAPM Task Group No. 105: issues associated with clinical implementation of Monte Carlo-based photon and electron external beam treatment planning. Med Phys. 2007;34:4818–53.
7. Gardner J, Sieberg J. Dose calculation validation of VMC++ for photon beams. Med Phys. 2007;34:1809–18.
8. Yamamoto T, Mizowaki T, Miyabe Y, Takegawa H, Narita Y, Yano S, Nagata Y, Teshima T, Hiraoka M. An integrated Monte Carlo dosimetric verification system for radiotherapy treatment planning. Phys Med Biol. 2007;52:1991–2008.
9. Okamoto H, Kanai T, Kase Y, Matsumoto Y, Furusawa Y, Fujita Y, Saitoh H, Itami J, Kohno T. Relation between linear energy distribution and relative biological effectiveness for photon beams according to the microdosimetric kinetic model. J Radiat Res. 2011;52:75–81.
10. Okamoto H, Kanai T, Kase Y, Matsumoto Y, Furusawa Y, Fujita Y, Saitoh H, Itami J, Kohno T. Microdosimetric study on the effect of low energy scattering photon for 6 MV therapeutic photon beams. Med Phys. 2011;38:4714–22.
11. Jiang H, Paganetti H. Adaptation of GEANT4 to Monte Carlo dose calculations based on CT data. Med Phys. 2004;31:2811–8.
12. Poon E, Verhaegen F. Accuracy of the photon and electron physics in GEANT4 for radiotherapy applications. Med Phys. 2005;32:1696–713.
13. Jan S, Benoit D, Becheva E, Carlier T, Cassol F, Descourt P, Frisson T, Grevillot L, Guigues L, Maigne L, Morel C, Perrot Y, Rehfeld N, Sarrut D, Schaart DR, Stute S, Pietrzyk U, Visvikis,

Zahra N, Buvat I. GATE V6: a major enhancement of the GATE simulation platform enabling modelling of CT and radiotherapy. Phys Med Biol. 2011;56(4):881–901.
14. Aso T, Kimura A, Kameoka S. Murakami K, Sasaki T, Yamashita T. GEANT4 based simulation framework for particle therapy system. In: Nucl Sci Symposium Conference Record. NSS'07. New York: IEEE; 2007. pp. 60–1.
15. Aso T, Maeda Y, Iwai G, Takase W, Sasaki T, Watase Y, Yamashita T, Akagi T, Nakano Y. Extension of the particle therapy simulation framework to hospital information systems and multigrid environments. In: IEEE International Conference Comput Eng (CSE2012), New York: IEEE Computer Society; 2012. pp. 229–34.
16. Heath E, Seuntjens J. Development and validation of a BEAMnrc component module for accurate Monte Carlo modelling of the varian dynamic millennium multileaf collimator. Phys Med Biol. 2003;48:4045–63.
17. Jang SY, Vassiliev ON, Liu HH, Mohan R, Siebers JV. Development and commissioning of a multileaf collimator model in Monte Carlo dose calculations for intensity-modulated radiation therapy. Med Phys. 2006;33:770–81.
18. Sievers JV, Keall PJ, Kim JO, Mohan R. A method for photon beam Monte Carlo multileaf collimator particle transport. Phys Med Biol. 2002;47:3225–49.
19. Huq MS, Das IJ, Steinberg T, Galvin JM. A dosimetric comparison of various multileaf collimators. Phys Med Biol. 2002;47:N159–70.
20. AAPM. Basic applications of multileaf collimators report of Task Group No. 50. American Association of Physicists in Medicine; 2001.
21. Graves MN, Thompson AV, Martel MK, McShan DL, Fraass BA. Calibration and quality assurance for rounded leaf-end MLC systems. Med Phys. 2001;28:2227–33.
22. Deng J, Pawlicki T, Chen Y, Li J, Jiang LSB, Ma C-M. The MLC tongue-and-groove effect on IMRT dose distributions. Phys Med Biol. 2001;46:1039–60.
23. Que W, Kung J, Dai J. 'Tongue-and-groove' effect in intensity modulated radiotherapy with static multileaf collimator fields. Phys Med Biol. 2004;49:399–405.
24. Tzedakis A, Damilakis JE, Mazonakis M, Stratakis J, Varveris H, Gourtsoyiannis N. Influence of initial electron beam parameters on Monte Carlo calculated absorbed dose distributions for radiotherapy photon beams. Med Phys. 2004;31:907–13.
25. Sheikh-Bagheri D, Rogers DWO. Monte Carlo calculation of nine mega-voltage photon beam spectra using the BEAM code. Med Phys. 2002;29:391–402.
26. Kawrakow I, Walters BRB. Efficient photon beam dose calculation using DOSXYZnrc with BEAMnrc. Med Phys. 2006;33:3046–56.
27. Dyk JV, Barnett RB, Cygler JE, Shragge PC. Commissioning and quality assurance of treatment planning computers. Int J Radiat Oncol Biol Phys. 1993;26:261–73.
28. Harms WB, Low DA, Wong JW, Purdy JA. A software tool for the quantitative evaluation of 3D dose calculations algorithms. Med Phys. 1998;10:1830–6.
29. Venselaar J, Welleweerd H. Application of a test package in an intercomparison of the photon dose calculation performance of treatment planning systems used in a clinical setting. Radiother Oncol. 2001;60:203–13.
30. Low DA, Harms WB, Mutic S, Purdy JA. A technique for the quantitative evaluation of dose distributions. Med Phys. 1998;25:656–61.
31. Low DA, Dempsey JF. Evaluation of the gamma dose distribution comparison method. Med Phys. 2003;30:2455–64.
32. Depuydt T, Esch AV, Huyskens DP. A quantitative evaluation of IMRT dose distributions: refinement and clinical assessment of the gamma evaluation. Radiot Oncol. 2002;62:309–19.
33. Kawachi T, Tohyama N, Kojima T, Kurooka M, Kito S, Okamoto H, Kumazaki Y, Hashimoto S, Fujita Y, Hayashi N. The dosimetric verification of IMRT. JSMP research report. 2010;30 supplement No. 6 (in Japanese).
34. Ulmer W, Harder D. A triple gaussian pencil beam model for photon beam treatment planning. Med Phys. 1995;5:25–30.
35. Ulmer W, Harder D. Application of a triple gaussian pencil beam model for photon beam treatment planning. Med Phys. 1996;6:68–74.

FULL PAPER

BJC

British Journal of Cancer (2015), 1–10 | doi: 10.1038/bjc.2014.623

Keywords: copy number increase of *ACTN4*; locally advanced pancreatic cancer; chemotherapy; chemoradiotherapy; predictive biomarker

ACTN4 copy number increase as a predictive biomarker for chemoradiotherapy of locally advanced pancreatic cancer

T Watanabe[1,2], H Ueno[3], Y Watabe[1], N Hiraoka[4], C Morizane[3], J Itami[5], T Okusaka[3], N Miura[1], T Kakizaki[1], T Kakuya[1], M Kamita[1], A Tsuchida[2], Y Nagakawa[2], H Wilber[6], T Yamada[1] and K Honda*[,1]

[1]*Division of Chemotherapy and Clinical Research, National Cancer Center Research Institute, 5-1-1, Tsukiji, Chuo-ku, Tokyo 104-0045, Japan;* [2]*Department of Gastrointestinal and Pediatric Surgery, Tokyo Medical University, Tokyo 160-0023, Japan;* [3]*Hepatobiliary and Pancreatic Oncology Division, National Cancer Center Hospital, Tokyo 104-0045, Japan;* [4]*Division of Molecular Pathology, National Cancer Center Research Institute, Tokyo, 104-0045 Japan;* [5]*Division of Radiation Oncology, National Cancer Center Research Institute, Tokyo 104-0045, Japan and* [6]*Abnova, 9th Floor, No. 108, Jhouzih Street, Neihu District, Taipei City 114, Taiwan*

Background: Several clinical trials have compared chemotherapy alone and chemoradiotherapy (CRT) for locally advanced pancreatic cancer (LAPC) treatment. However, predictive biomarkers for optimal therapy of LAPC remain to be identified. We retrospectively estimated amplification of the *ACTN4* gene to determine its usefulness as a predictive biomarker for LAPC.

Methods: The copy number of *ACTN4* in 91 biopsy specimens of LAPC before treatment was evaluated using fluorescence *in situ* hybridisation (FISH).

Results: There were no statistically significant differences in overall survival (OS) or progression-free survival (PFS) of LAPC between patients treated with chemotherapy alone or with CRT. In a subgroup analysis of patients treated with CRT, patients with a copy number increase (CNI) of *ACTN4* had a worse prognosis of OS than those with a normal copy number (NCN) of *ACTN4* ($P=0.0005$, log-rank test). However, OS in the subgroup treated with chemotherapy alone was not significantly different between patients with a CNI and a NCN of *ACTN4*. In the patients with a NCN of *ACTN4*, the median survival time of PFS in CRT-treated patients was longer than that of patients treated with chemotherapy alone ($P=0.049$).

Conclusions: The copy number of *ACTN4* is a predictive biomarker for CRT of LAPC.

Despite progress in clinical cancer medicine in the fields of imaging technology, surgical management, therapeutic modalities and molecular-targeted therapy, the prognosis of pancreatic cancer has remained dismal. Every year in Japan, ~27 000 patients are diagnosed with pancreatic cancer, with almost the same number dying from this disease (Mayahara *et al*, 2012). Indeed, the 5-year overall survival (OS) rate of patients with pancreatic cancer is ⩽5% (Johung *et al*, 2012).

Locally advanced pancreatic cancer (LPAC) is defined as a surgically unresectable disease without detectable metastasis. Effective therapy for patients with LAPC is not only crucial for any hope of long-term survival, but also necessary for symptom management. Because survival rates for patients with LAPC are generally low, treatment recommendations often involve aggressive multimodal therapies (Savir *et al*, 2013). A multidisciplinary approach involving surgical oncologists, medical oncologists and radiation oncologists is strongly recommended for balanced discussion of management options (Pawlik *et al*, 2008; Katz *et al*, 2013; Mian *et al*, 2014).

At present, treatment options for LAPC include chemotherapy alone, induction chemotherapy followed by chemoradiotherapy (CRT) or definitive CRT. Numerous randomised trials have been

*Correspondence: Professor K Honda; E-mail: khonda@ncc.go.jp

Received 24 August 2014; revised 31 October 2014; accepted 25 November 2014

performed to compare the survival benefit between chemotherapy alone and CRT for LAPC (Chauffert *et al*, 2008; Loehrer *et al*, 2011). Nevertheless, as there are some contradictory results, the most effective treatment has not yet been defined for patients with LAPC (Savir *et al*, 2013; Mian *et al*, 2014). Radiotherapy focussed on the primary site does not have a direct impact on distant metastatic lesions and radiotherapy should therefore be limited to patients without metastases (Berger *et al*, 2008). If pancreatic cancer oncologists can accurately evaluate the occult distant metastasis before deciding the therapeutic strategy, they should be able to choose the optimal therapy for individual patients with LAPC. However, it is not yet possible to accurately detect micrometastatic lesions using imaging technology. Therefore, elucidation of biomarkers that can accurately evaluate metastatic potential from biopsy samples obtained from patients with LAPC is very important for deciding the best personalised therapeutic strategy from multimodal therapies.

In 1998, we identified actinin-4 (gene name *ACTN4*) as an actin-binding protein that is closely associated with cancer invasion and metastasis (Honda *et al*, 1998; Hayashida *et al*, 2005). Immunohistochemical analysis (IHC) showed that overexpression of the actinin-4 protein was significantly correlated with a poor prognosis for breast (Honda *et al*, 1998), pancreas (Kikuchi *et al*, 2008), ovary (Yamamoto *et al*, 2007, 2009, 2012) and lung cancer (Miyanaga *et al*, 2013; Noro *et al*, 2013).

We subsequently found that gene amplification of *ACTN4*, which is the gene name of the actinin-4 protein, is responsible for overexpression of the actinin-4 protein in a number of pancreatic cancer patients (Kikuchi *et al*, 2008). Using fluorescence *in situ* hybridisation (FISH), we then reported that gene amplification of *ACTN4* is a good biomarker for identification of patients with a poor prognosis for ovarian cancer (Yamamoto *et al*, 2009), salivary gland carcinoma (Watabe *et al*, 2014) and stage-I adenocarcinoma of the lung (Noro *et al*, 2013).

In this study, we retrospectively investigated the status of actinin-4 protein expression and *ACTN4* copy number in biopsy samples of LAPC patients. We confirmed the possibility that *ACTN4* copy number is useful as a predictive and prognostic biomarker of CRT for LAPC.

MATERIALS AND METHODS

Patients. A total of 91 patients who were diagnosed as having LAPC from May 2001 until December 2003 underwent chemotherapy alone or CRT at the National Cancer Center Central Hospital (Tokyo, Japan). All patients were diagnosed as adenocarcinoma of the pancreas by fine needle biopsy. This study was reviewed and approved by the institutional ethical committee and informed consent was obtained from the patients for this study.

At first diagnosis, multidetector computed tomography (CT) involving the chest and abdomen was performed for assessment of the local extension of the primary tumour, and for exclusion of distant metastasis. The CT-based criteria regarding tumour unresectability included enhancement or occlusion of the coeliac trunk, common hepatic artery, superior mesenteric artery or aorta (Ikeda *et al*, 2007; Mayahara *et al*, 2012).

Immunohistochemistry. Formalin-fixed, paraffin-embedded (FFPE) pathology blocks, which were made to diagnose the biopsy specimens, were cut into 4 μm-thick sections.

An anti-actinin-4 monoclonal antibody was established by our group (Miyanaga *et al*, 2013; Noro *et al*, 2013) (Abnova, Taipei, Taiwan). Immunostaining of actinin-4 was performed using the Ventana DABMap detection kit and an automated slide stainer (Discovery XT; Ventana Medical System, Tucson, AZ, USA) (Watabe *et al*, 2014). The immunohistochemical staining of actinin-4 was classified into two groups: positive and negative. Positive was defined as strong protein expression of actinin-4 in the cytoplasm and cell membranes of cancer cells. Negative was defined as no detection of actinin-4 protein in cancer cells or weak expression of actinin-4 in the cytoplasm or cell membrane of cancer cells (Figure 1). Two independent investigators (TW and YW) who had no clinical information about these cases evaluated the staining pattern.

Fluorescence *in situ* hybridisation. The FISH probes of the bacterial artificial chromosome (BAC) clone containing *ACTN4* were prepared by our group (Noro *et al*, 2013) (Abnova). The labelled BAC clone DNA was subjected to FISH as previously described. Sections that were cut from an FFPE biopsy block (4 μm thick) were hybridised with FISH probes at 37 °C for 48 h. The nuclei were counterstained with 4,6-duamidino-2-phenylindone. The number of fluorescence signals corresponding to the copy number of *ACTN4* in the nuclei of 20 interphase tumour cells was counted (TW and YW) (Watabe *et al*, 2014).

The FISH patterns were defined as described previously. Briefly, the biopsy samples were grouped as normal copy number (NCN) (two or fewer *ACTN4* signals in $>90\%$ of cells) and copy number increase (CNI) (four or more *ACTN4* signals in $>10\%$ of the tumour cells) (Figure 1) (Watabe *et al*, 2014).

Statistical analysis. Significant correlations were detected by using Fisher's exact test. Overall survival and progression-free survival (PFS) were measured as the period from first diagnosis to the event or last follow-up and were estimated by Kaplan–Meier analysis. Significant differences between curves of OS or PFS were assessed using the log-rank test. Univariate and multivariate analyses for death were performed using the Cox regression model. Data were analysed using the StatFlex statistical software package (version 6.0; Artiteck, Osaka, Japan) or the R-project (http://www.r-project.org/) (Honda *et al*, 2005, 2012; Noro *et al*, 2013).

RESULTS

Patient characteristics and survival benefit comparison between chemotherapy alone and CRT. In all, 34 patients with LAPC underwent chemotherapy alone. The regimens of chemotherapy alone comprised gemcitabine (GEM) alone ($n=29$), combination of GEM and erlotinib ($n=1$), combination of GEM and S-1 ($n=3$) or S-1 alone ($n=1$). A total of 57 patients with LAPC underwent CRT. The regimens of CRT comprised radiotherapy (RT) and 5-fluorouracil (5-FU) ($n=39$), RT and GEM ($n=10$) and RT and S-1 ($n=8$). The median age of patients and tumour size for all of the cases was 63.0 years and 37.4 mm, respectively. Statistical significances of patient characteristics with respect to age, gender, Eastern Cooperative Oncology Group Performance Status (PS), tumour size, lymph node metastasis and location of tumours were calculated. No statistically significant differences were observed between any of these factors and chemotherapy alone or CRT (Table 1).

The statistical significance of differences between the benefit of chemotherapy alone and that of CRT for OS and PFS was also calculated. In the absence of biomarker selection, no statistically significant differences in survival benefits in terms of OS and PFS were found between patients treated with chemotherapy alone and those treated with CRT (Figure 2).

Prognostic impact of protein expression of actinin-4 in patients with LAPC. We previously showed that protein overexpression of actinin-4 is a prognostic biomarker for resectable invasive ductal adenocarcinoma of the pancreas (Kikuchi *et al*, 2007). We investigated the protein expression level of actinin-4 in LAPC by using IHC. The 91 patients with LAPC were classified into one

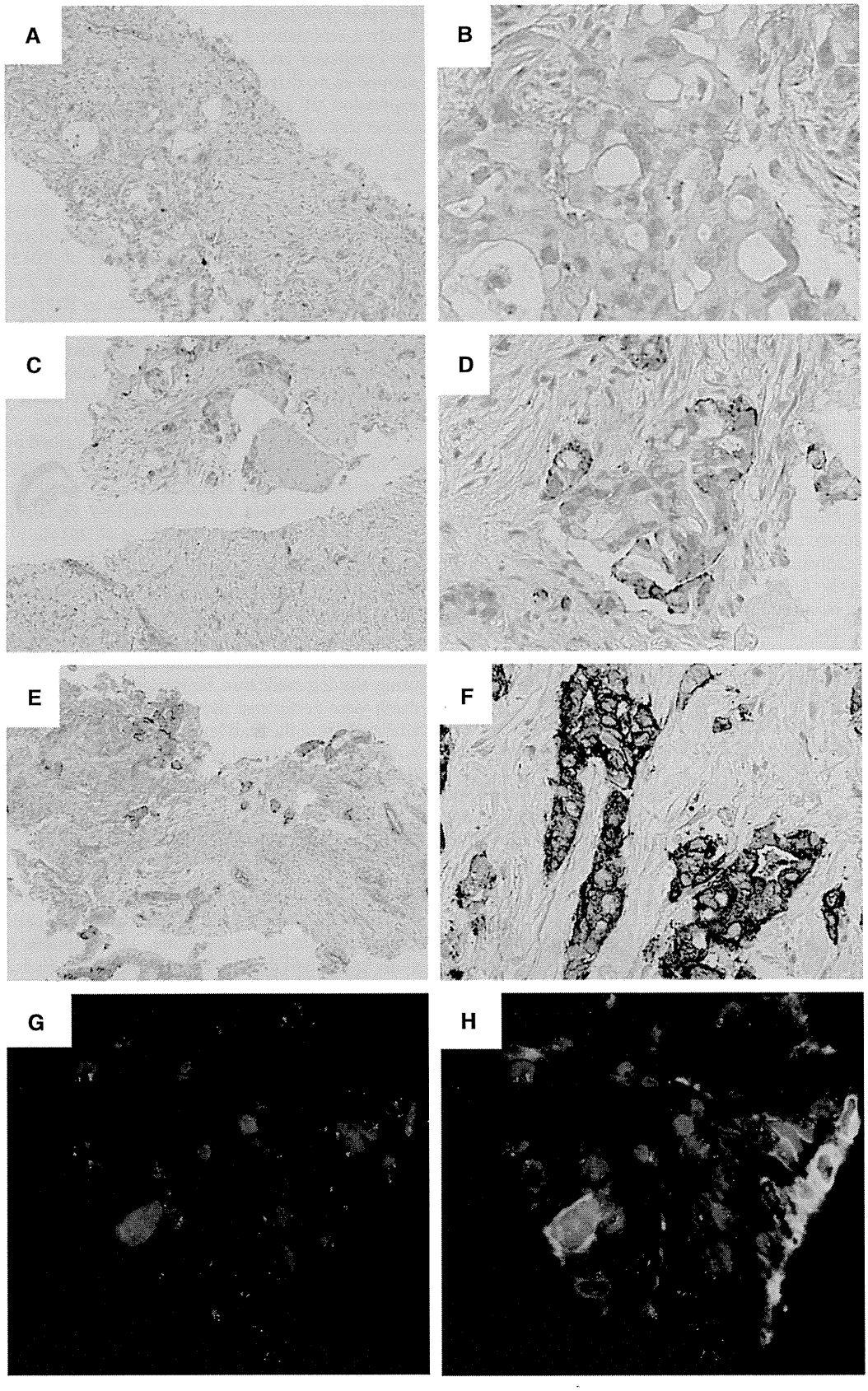

Figure 1. Immunohistochemical (IHC) and fluorescence *in situ* hybridisation (FISH) analyses of representative actinin-4 protein expression and *ACTN4* copy number, respectively, in LAPC biopsy specimens. (**A–F**) Immunohistochemical analysis of actinin-4 protein expression. Representative cases of no expression (**A**, **B**), weak expression (**C**, **D**) and strong expression (**E**, **F**) of actinin-4 protein in LAPC cells. (**A**), (**C**) and (**E**) are low-magnitude images. (**B**), (**D**) and (**F**) are high-magnitude images of regions of (**A**), (**C**) and (**E**), respectively. (**G**, **H**) Fluorescence *in situ* hybridisation analysis of representative cases with a copy number increase (CNI) in *ACTN4*.

Table 1. Baseline patient characteristics

	Total		CRT		CT		
Characteristic	**Number**	**%**	**Number**	**%**	**Number**	**%**	***P*-value***
Median age, years (63.0)							0.0501
<63.0	45	49.5	32	56.1	13	38.2	
⩾63.0	46	50.5	25	43.9	21	61.8	
Gender							1
Male	53	58.2	33	57.9	20	58.8	
Female	38	41.8	24	42.1	14	41.2	
PS							0.2681
0	26	28.6	17	29.8	9	26.5	
1	63	69.2	40	70.2	23	67.6	
2	2	2.2	0	0.0	2	5.9	
Median tumour size, mm (37.4)							0.3862
<37.4 mm	44	48.4	14	41.2	30	52.6	
⩾37.4 mm	47	51.6	20	58.8	27	47.4	
Lymph node metastasis							1
Negative	64	70.3	40	70.2	24	70.6	
Positive	27	29.7	17	29.8	10	29.4	
Location of the tumour							0.0501
Head of pancreas	43	47.3	22	38.6	21	61.8	
Body or tail of pancreas	48	52.7	35	61.4	13	38.2	
CA19-9							
<1000 U ml^{-1}	62	68.1	39	68.4	23	67.6	1
⩾1000 U ml^{-1}	29	31.9	18	31.6	11	32.4	

Abbreviations: CRT = chemoradiotherapy; CT = chemotherapy; PS = Eastern Cooperative Oncology Group Performance Status. *P-value: Fisher's exact test (two sided).

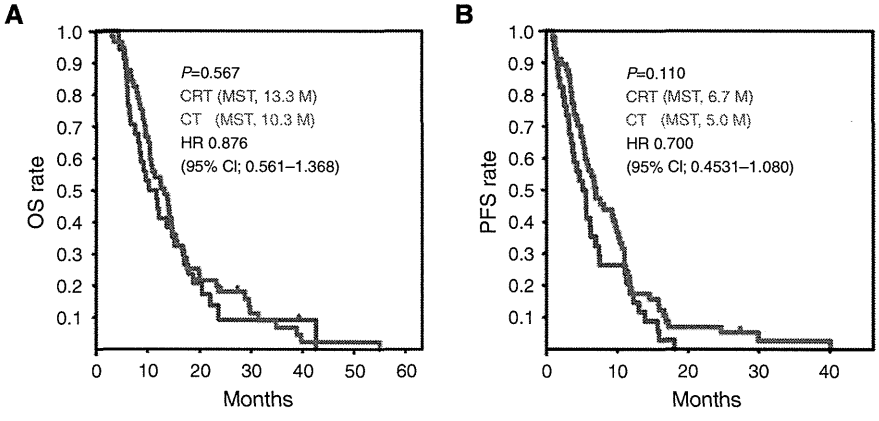

Figure 2. Kaplan–Meier analyses of overall survival (OS) and progression-free survival (PFS) in all locally advanced pancreatic cancer (LAPC) cases. The survival curves of all LAPC patients treated with chemotherapy alone (CT, blue lines) or with chemoradiotherapy (CRT, red lines) are shown. Statistically significant differences in OS (**A**) and PFS (**B**) were calculated using a log-rank test. Median survival time (MST) is shown in months (M). The clinical benefit of CT *vs* CRT was calculated by univariate Cox regression analysis (hazard ratio (HR) and 95% confidence interval (95% CI)). The y axis is the rate of OS or PFS, and the x axis is the time after first diagnosis (months).

of two groups based on actinin-4 protein expression; positive (66 patients, 72.5%) and negative (25 patients, 27.5%). We investigated correlations between protein expression of actinin-4 and the following patient characteristics: age, gender, PS, size of tumour, lymph node metastasis and treatment strategy (chemotherapy alone or CRT). Protein expression of actinin-4 was statistically correlated with tumour location ($P = 0.0379$; Table 2).

We determined whether protein expression of actinin-4 provided benefit for OS to patients with LAPC by comparing the OS of cases of LAPC with and without actinin-4 expression (total, $n = 91$). No statistically significant difference in OS between actinin-4 protein-positive and -negative cases was found ($P = 0.116$, log-rank test; Figure 3A). However, although a statistical significance was not found by Kaplan–Meier analysis, the median survival time (MST) of OS of cases positive for acitinin-4 protein was 10.9 months, which was shorter than the MST of the negative cases (14.8 months) by 3.9 months (Figure 3A).

Determination of the copy number of *ACTN4* by FISH, and prognostic impact of copy number of *ACTN4* for LAPC. It is known that gene amplification of *ACTN4* is responsible for

Table 2. Association of protein expression of actinin-4 and copy number increase in *ACTN4* with clinicopathological characteristics of locally advanced pancreatic cancer

	Actinin-4 IHC					*ACTN4* FISH				
Characteristic	**Positive**	**%**	**Negative**	**%**	***P*-value***	**Positive**	**%**	**Negative**	**%**	***P*-value***
Median age, years (63.0)					0.159					0.41
<63.0	36	54.5	9	36.0		9	60.0	36	47.4	
⩾63.0	30	45.5	16	64.0		6	40.0	40	52.6	
Gender					0.6348					**0.02**
Male	37	56.1	16	64.0		13	86.7	40	52.6	
Female	29	43.9	9	36.0		2	13.3	36	47.4	
PS					0.3506					0.679
0	21	31.8	5	20.0		3	20.0	23	30.3	
1	44	66.7	19	76.0		12	80.0	51	67.1	
2	1	1.5	1	4.0		0	0.0	2	2.6	
Tumour size					0.8647					1
<37.4 mm	33	50.0	12	48.0		7	46.7	38	50.0	
⩾37.4 mm	33	50.0	13	52.0		8	53.3	38	50.0	
Lymph node metastasis					0.4478					0.059
Negative	48	72.7	16	64.0		7	46.7	57	75.0	
Positive	18	27.3	9	36.0		8	53.3	19	25.0	
Location of the tumour					**0.0379**					0.156
Head of pancreas	31	47.0	18	72.0		10	66.7	33	43.4	
Body or tail of pancreas	35	53.0	7	28.0		5	33.3	43	56.6	
CA19-9					0.451					0.227
$<1000\,U\,ml^{-1}$	43	65.2	19	76.0		8	53.3	54	71.1	
$\geqslant 1000\,U\,ml^{-1}$	23	34.8	6	24.0		7	46.7	22	28.9	
Therapy					1					1
CT	25	37.9	9	36.0		6	40.0	28	36.8	
CRT	41	62.1	16	64.0		9	60.0	48	63.2	

Abbreviations: *ACTN4* = *actinin-4*; CRT = chemoradiotherapy; CT = chemotherapy; FISH = fluorescence *in situ* hybridisation; IHC = immunohistochemistry; PS = Eastern Cooperative Oncology Group Performance Status. **P*-value: Fisher's exact test (two sided). Bold entries indicate statistically significance.

overexpression of actinin-4 protein in a number of patients with pancreatic cancer. In addition, gene amplification of *ACTN4* predicts a poorer prognosis than protein overexpression of actinin-4 in ovarian (Yamamoto *et al*, 2009), lung (Noro *et al*, 2013) and salivary gland cancer (Watabe *et al*, 2014). To evaluate the significance of *ACTN4* as a prognostic factor for LAPC, we determined the copy number of *ACTN4* in patients with LAPC by FISH. Of the 91 LAPC patients whom we examined, 76 patients were classified as NCN (83.5%) and 15 patients were classified as CNI (16.5%). Although only 1 of the 25 cases who were negative for actinin-4 protein (4.0%) had a CNI of *ACTN4*, 14 of the 66 cases who were actinin-4 protein positive (21.2%) had a CNI of *ACTN4* (Table 3). We also analysed association of the *ACTN4* copy number, as assessed by FISH analysis, with clinicopathological characteristics. There were statistically significant differences between gender and copy number of *ACTN4* ($P=0.02$; Table 2).

When all cases of LAPC were considered, the difference in OS between cases with a CNI and those with NCN of *ACTN4* was statistically significant ($P=0.0019$, log-rank test). The MST of OS in the cases with a CNI of *ACTN4* (8.7 months) was also significantly shorter than the MST of NCN cases (13.7 months) by 5 months ($P=0.0019$; Figure 3B).

Prognostic impact of the serum level of CA19-9 in patients with LAPC. The serum level of CA19-9 has been reported to be a prognostic factor for patients with LAPC (Berger *et al*, 2008; Mayahara *et al*, 2012; Yang *et al*, 2013). We confirmed the usefulness of the serum level of CA19-9 as a prognostic factor for patients with LAPC in our study. The LAPC patients were classified into one of two groups: CA19-9 high expression ($\geqslant 1000\,U\,ml^{-1}$) and CA19-9 low–intermediate expression ($<1000\,U\,ml^{-1}$), as previously described (Mayahara *et al*, 2012). There was a statistically significant difference in OS between the CA19-9 high-expression group and the CA19-9 low–intermediate-expression group ($P=0.0003$, log-rank test; Supplementary Figure 1). The MST of the CA19-9 high-expression group was 9.3 months, which was shorter than the MST of the CA19-9 low–intermediate-expression group (14.6 months) by 5.3 months.

Univariate analysis indicated that the risk factors for death of LAPC patients were: lymph node metastasis, serum level of CA19-9 (cutoff value; $1000\,U\,ml^{-1}$) and copy number status of *ACTN4*. The hazard ratios (HRs) for the death of patients with LAPC of lymph node metastasis, CA19-9 and a CNI of *ACTN4* were: 1.606 (95% confidence interval (CI); 1.008–2.560, $P=0.0463$), 2.354 (95% CI; 1.479–3.761, $P=0.0003$) and 2.531 (95% CI; 1.394–4.597, $P=0.0023$), respectively. By multivariate analysis, the serum level of CA19-9 (HR; 2.325, 95% CI; 1.416–3.818, $P=0.0009$) and a CNI of *ACTN4* (HR; 2.645, 95% CI; 1.439–4.861, $P=0.0017$) were independent risk factors for the death of patients with LAPC. The HR of CNI of *ACTN4* (HR; 2.531) was slightly higher than that of the serum level of CA19-9 (HR; 2.354; Table 4).

Evaluation of OS in subgroup analyses of treatment strategy with copy number of *ACTN4*. A biomarker that can evaluate the potential for metastatic activity in tumour cells has the possibility of use as a predictive biomarker of CRT. It is known that *ACTN4* is an oncogene that is associated with cancer metastasis and cell invasion. In order to evaluate the benefit for OS based on the copy

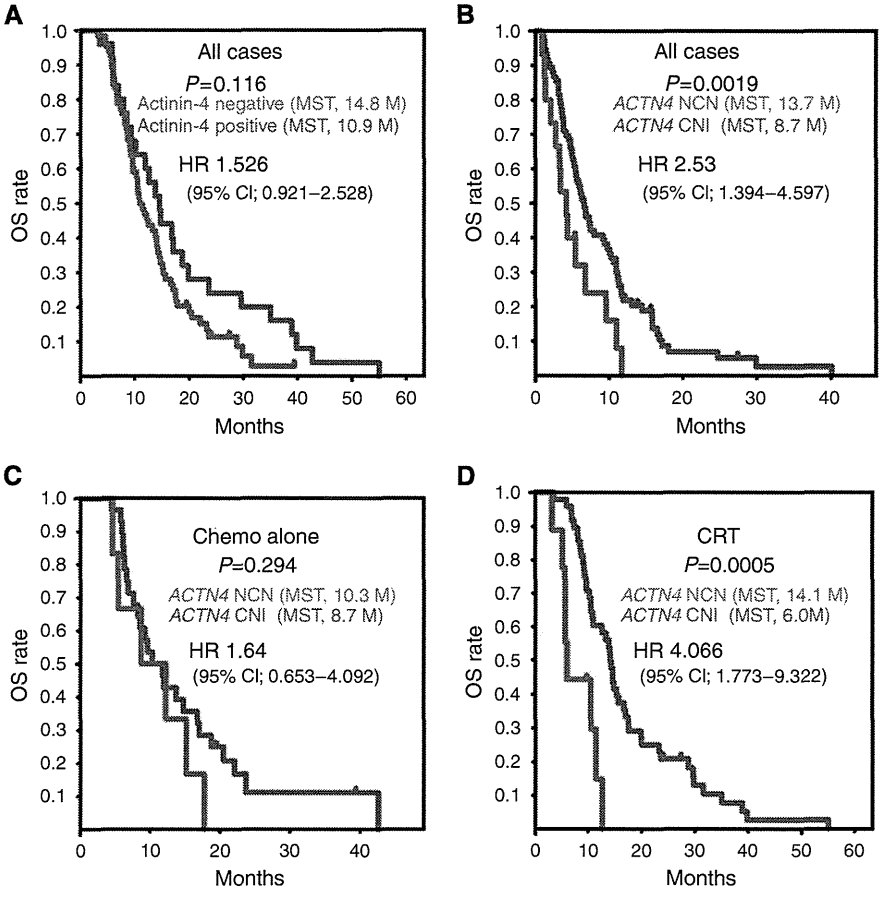

Figure 3. Kaplan–Meier analyses of survival relative to protein expression of actinin-4 and copy number of *ACTN4*. (**A**) Overall survival (OS) curves based on protein expression of actinin-4. The blue line represents patients with negative expression of actinin-4. The red line represents patients with positive expression of actinin-4. (**B–D**) The OS curves based on *ACTN4* copy number status in all cases ($n=91$) (**B**), in the subgroup treated with chemotherapy alone (Chemo alone, $n=34$) (**C**) and in the chemoradiotherapy (CRT)-treated subgroup ($n=57$) (**D**). The blue lines represent patients who were evaluated as normal copy number (NCN) of *ACTN4*. The red lines represent patients who were evaluated as copy number increase (CNI) of *ACTN4*. Statistical parameters were calculated as described for Figure 2. The y axis is the rate of OS, and the x axis is the time after first diagnosis (months).

Table 3. Statistical analysis of the association between the status of protein expression of actinin-4 and the copy number of *ACTN4*

	Copy number status of *ACTN4*			
Status of actinin-4 with IHC	**NCN (%)**	**CNI (%)**	**Total**	***P*-value***
Negative	24 (96.0)	1 (4.0)	25	**0.042**
Positive	52 (78.8)	14 (21.2)	66	
Total	76 (83.5)	15 (16.5)	91	

Abbreviations: *ACTN4* = *actinin-4*; CNI = copy number increase; IHC = immunohistochemistry; NCN = normal copy number. **P*-value: Fisher's exact test (one sided). Bold entry indicates statistically significance.

number status of *ACTN4* for each treatment strategy, the patients with LAPC were classified into one of two subgroups on the basis of treatment strategies: a chemotherapy-alone group and a CRT group. We then analysed the impact of the copy number status of *ACTN4* on OS of each subgroup. No statistical significance was observed between OS of patients with a NCN and with a CNI of *ACTN4* in the chemotherapy-alone subgroup ($P=0.294$, log-rank test). The MST of CNI and NCN of *ACTN4* patients was almost the same at 8.7 and 10.3 months, respectively (Figure 3C). Univariate Cox regression analysis indicated that the HR for death of CNI patients compared with NCN patients was 1.64 (95% CI; 0.653–4.092) in the chemotherapy-alone subgroup, and no statistically significant difference was found between CNI and NCN patients in the chemotherapy-alone subgroup ($P=0.291$).

In contrast, in the subgroup who underwent CRT, the OS of CNI of *ACTN4* patients was significantly worse than that of patients with a NCN ($P=0.0005$, log-rank test), and the MST of CNI of *ACTN4* patients (6.0 months) was definitely shorter than that of NCN of *ACTN4* patients (14.1 months; Figure 3D). Univariate Cox regression analysis of the CRT groups indicated that the HR for death of CNI patients compared with that for NCN patients was 4.066 (95% CI; 1.773–9.322), and the difference between CNI and NCN groups was statistically significant ($P=0.0009$). The HR for death in the comparison between CNI and NCN of *ACTN4* (4.066) patients in the CRT subgroup was higher than that of the HR in the comparison between the CNI and NCN of *ACTN4* patients in all 91 cases (HR; 2.531; Table 4).

We also calculated the prognostic impact of the serum level of CA19-9 in each subgroup of therapeutic strategy on OS. The OS of patients with high expression of CA19-9 was significantly worse than that of patients with low–intermediate expression of CA19-9 in both subgroups of the chemotherapy-alone group ($P=0.00218$, log-rank test; Supplementary Figure 2) and the CRT group ($P=0.0095$; Supplementary Figure 3).

Table 4. Univariate and multivariate Cox proportional hazard models to predict survival of patients with locally advanced pancreatic cancer receiving chemotherapy or chemoradiotherapy

	Univariate analysis			Multivariate analysis		
	HR	95% CI	*P*-value	HR	95% CI	*P*-value
Median age, years (63.0)						
<63.0/⩾63.0	0.959	0.624–1.474	0.8498			
Gender						
Male/female	0.802	0.519–1.249	0.334			
PS						
0/1 and 2	1.126	0.697–1.819	0.6270			
Median tumour size, mm (37.4)						
<37.4 mm/⩾37.4 mm	1.066	0.665–1.709	0.7902			
Lymph node metastasis						
Negative/positive	**1.606**	**1.008–2.560**	**0.0463**	1.199	0.7654–1.978	0.0740
Location of the tumour						
Head/body or tail of pancreas	0.764	0.492–1.185	0.2294			
CA19-9						
<1000/⩾1000 U ml^{-1}	**2.354**	**1.479–3.761**	**0.0003**	**2.325**	**1.416–3.818**	**0.0009**
Actinin-4 IHC						
Negative/positive	1.526	0.922–2.528	0.1004			
***ACTN4* FISH**						
NCN/CNI	**2.531**	**1.394–4.597**	**0.0023**	**2.645**	**1.439–4.861**	**0.0017**

Abbreviations: *ACTN4* = *actinin-4*; 95% CI = 95% confidence interval; CNI = copy number increase; FISH = fluorescence *in situ* hybridisation; HR = hazard ratio; IHC = immunohistochemistry; NCN = normal copy number; PS = Eastern Cooperative Oncology Group Performance Status. Bold entries indicate statistically significance.

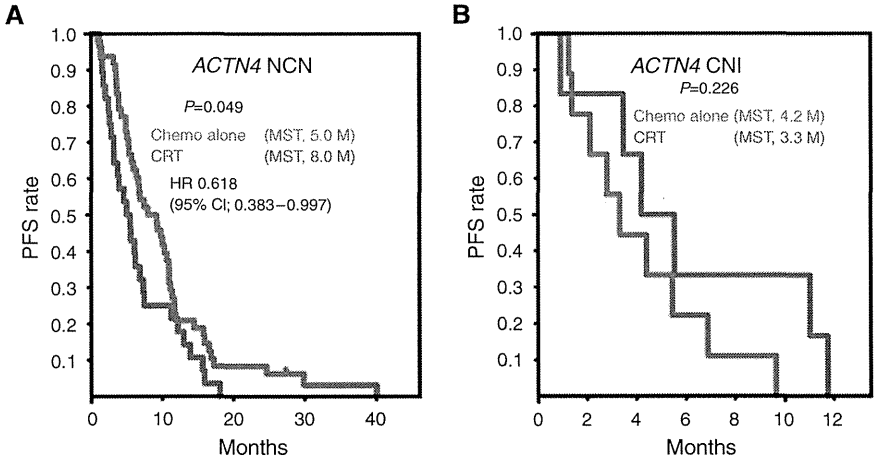

Figure 4. Kaplan–Meier analyses of progression-free survival (PFS) in CNI and NCN subgroups of *ACTN4*. The PFS curves of patients with a NCN of *ACTN4* (**A**) or a CNI of *ACTN4* (**B**), treated with chemotherapy alone (chemo alone, blue line) or with chemoradiotherapy (CRT, red line). The y axis is the rate of PFS and the x axis is the time after first diagnosis (months). Statistical parameters were calculated as described for Figure 2.

The benefit for PFS of CRT-treated patients who were selected by copy number status of *ACTN4*. We further examined the ability of *ACTN4* copy number to function as a predictive biomarker for CRT using subgroup analysis of the copy number status of *ACTN4*. We classified the patients into CNI and NCI subgroups of *ACTN4* and compared PFS in these CNI and NCI subgroups of *ACTN4* patients between the two arms of chemotherapy alone and CRT. Kaplan–Meier analysis indicated a statistically significant difference in the PFS of NCN patients in the chemotherapy-alone group compared with that of the CRT subgroup ($P = 0.049$; Figure 4A). The median PFS of the patients who were evaluated as NCN of *ACTN4* in the CRT subgroup was 8.0 months, whereas that for NCN of *ACTN4* patients in the chemotherapy-alone subgroup was 5.0 months. Thus, the median PFS of patients with NCN of *ACTN4* in the CRT subgroup was longer than that of patients with NCN of *ACTN4* in the chemotherapy-alone subgroup by 3 months. The HR for tumour progression of patients with NCN of *ACTN4* in the CRT subgroup compared with the chemotherapy-alone subgroup was 0.618 (95% CI; 0.383–0.997). No statistically significant difference in the PFS of patients with a CNI of *ACTN4* was noted between the chemotherapy-alone and the CRT subgroups ($P = 0.226$; Figure 4B). However, the MST of PFS in patients with a CNI of *ACTN4* in the chemotherapy-alone subgroup (4.2 months) was slightly longer (0.9 month longer) than that of patients with a CNI of *ACTN4* in the CRT subgroup (3.3 months). For both cohorts, there were no statistically significant differences in OS between the chemotherapy-alone and the CRT subgroups (data not shown).

DISCUSSION

In this study, we demonstrated that CNI of *ACTN4* is a predictive biomarker for the therapeutic strategy of LAPC. Although there have been a large number of studies and trials regarding the best chemotherapeutic strategy for extension of survival of patients with LAPC (Colucci *et al*, 2002; Huguet *et al*, 2007; Moore *et al*, 2007; Chauffert *et al*, 2008; Loehrer *et al*, 2011), the optimal therapy for patients with LAPC has not yet been decided upon. Clinical trials have reported contradictory results. Thus, the ECOG E4201, FFCD/SFRO and LAP07 phase III trials reported that the MST of OS in patients who received CRT was improved (Loehrer *et al*, 2011), decreased (Chauffert *et al*, 2008) or showed no statistically significant survival benefit compared with patients who received chemotherapy alone. The results of these studies suggest that there is a potential benefit to selecting appropriate patients for intensified treatment.

In order to select either chemotherapy or CRT as a treatment strategy, the metastatic potential of the tumour itself needs to be accurately evaluated. This is because radiotherapy can only exert a direct physicochemical effect on the tumour at the primary tumour site that is exposed to radiation, whereas chemotherapy can access both the primary tumour and distant metastasis. Therefore, patients with latent metastatic lesions, including lesions that cannot be detected using modern technology, should receive only strong chemotherapy, whereas patients who definitely have no distant metastatic lesions before initial treatment should receive CRT in order to exert sufficient physicochemical impact on the primary tumour site. Our finding that *ACTN4* copy number is a predictive marker for selection of therapy for LAPC should therefore prove valuable for optimisation of treatment strategy and help to provide the maximum personalised medicine for individual patients. Other predictive markers for treatment selection strategy have been suggested. Smad4 (Dpc4) is a tumour-suppressor gene involved in cell motility that is inactivated in 53% of pancreatic cancers. Prospective validation of smad4 expression in cytological specimens suggested that smad4 may be a predictive biomarker, and that analysis of smad4 levels may lead to personalised treatment strategies for patients with LAPC (Crane *et al*, 2011).

In the present paper we could not find any statistically significant difference in OS or PFS between LAPC patients who were treated with either chemotherapy alone or with CRT (Figure 2), again suggesting the need for a predictive marker for selection of patients for specific treatment. The potential predictive marker we considered was gene amplification of ACTN4.

The *ACTN4* gene encodes the actinin-4 protein, an actin-bundling protein that was isolated by our group in 1998 (Honda *et al*, 1998). Its protein overexpression is closely associated with cancer invasion and cell motility. Actinin-4 has one actin-binding domain at the N-terminus, and actinin-4 monomers can form a homodimer by binding in the opposite direction to form a dumbbell-shaped structure (Otey and Carpen, 2004). The actinin-4 homodimer can strongly bind F-actin and subsequently form bundling F-actin. Moreover, the bundling F-actin formed by actinin-4 makes strong contact with the cell membrane, following which cellular protrusions that are associated with cell motility are formed on the cell membrane (Welsch *et al*, 2009). The protein overexpression of actinin-4 in cancer cells stimulates dynamic remodelling of the actin cytoskeleton, and it is for this reason that actinin-4-overexpressing cancer cells have metastatic potential (Hayashida *et al*, 2005). Indeed, there are some reports that patients with cancers showing protein overexpression of actinin-4 have significantly worse OS than patients with cancers who are negative for actinin-4 (Honda *et al*, 1998; Yamamoto *et al*, 2007; Noro *et al*, 2013). Moreover, Kikuchi *et al* (2008) reported that protein overexpression of actinin-4 was a poor prognostic factor for invasive ductal adenocarcinoma of the pancreas. However, in the present study we could not find a statistically significant positive correlation between actinin-4 protein overexpression and poor prognosis. One difference between our present study and the previous study of Kikuchi *et al* (2008) was that in the latter study protein expression of actinin-4 was immunohistochemically evaluated using whole pathological sections that were obtained from surgical samples, whereas in the present study protein expression of actinin-4 was immunohistochemically evaluated using biopsy specimens of LAPC. In the study of Kikuchi *et al* (2008), the staining pattern of endothelial cells as an internal control was used to accurately evaluate the protein expression level of actinin-4 in tumour cells. However, accurate evaluation of the protein expression level of actinin-4 from biopsy specimens was more difficult than from whole pathological sections because the biopsy specimens did not always include endothelial cells. These technical problems may therefore explain the difference in the results of the two studies. One cause of protein overexpression of actinin-4 in cancer cells is amplification of the *ACTN4* gene (Kikuchi *et al*, 2008) and it has been reported that the CNI of *ACTN4* is a better prognostic predictor than protein expression of actinin-4 (Yamamoto *et al*, 2009; Noro *et al*, 2013; Watabe *et al*, 2014). We found a statistically significant difference in OS between patients with a CNI and those with a NCN, and patients with a CNI had a worse prognosis in terms of OS than NCN patients (Figure 3B). Furthermore, multivariate Cox regression analysis indicated that a CNI of *ACTN4* and high serum CA19-9 levels were independent prognostic factors for the death of patients, and that the HR of CNI of *ACTN4* was higher than that of high CA19-9 levels (Table 4). These data confirmed the usefulness of CA19-9 as a prognostic factor for LAPC and further suggested that *ACTN4* might be a prognostic factor for LAPC.

Subgroup analyses of CNI and NCN patients who were treated with chemotherapy alone or with CRT using FISH to calculate *ACTN4* copy number showed that whereas the copy number of *ACTN4* may be a predictive biomarker for CRT of LAPC, CA19-9 was not a predictive biomarker for either chemotherapy alone or CRT. Thus, there was no statistically significant difference in OS between CNI and NCN patients in the subgroup who were treated with chemotherapy alone (Figure 3C). However, in the subgroup of patients who were treated with CRT, the CNI patients with an MST of 14.1 months had a significantly longer survival time than NCN patients who had an MST of 6.0 months (Figure 3D). In contrast, serum CA19-9 levels showed statistically significant differences in terms of OS for both subgroups (Supplementary Figures 1–3).

Our data further confirmed the usefulness of *ACTN4* as a predictive biomarker for CRT in the study of the PFS of patients with LAPC who were classified into CNI and NCN of *ACTN4* groups and were then further classified into subgroups based on therapeutic strategies. We found a statistically significant difference in good prognosis of PFS between the NCN group treated with CRT (MST of PFS of 8.0 months) compared with the NCN group treated with chemotherapy alone (5.0 months; Figure 4A). Interestingly, although no statistically significant difference in PFS was found between the subgroups of CNI of *ACTN4* who were treated with chemotherapy alone or with CRT, the MST of PFS was the reverse of that seen in the NCN group, with the MST of chemotherapy alone being 4.2 months and that of CRT being shorter at 3.3 months. These data suggest that, when considering therapy for LAPC patients, patients with a NCN of *ACTN4* should at least undergo CRT (Figure 4B). However, no statistically significant difference in benefit in OS was noted in subgroup analysis of CNI and NCN of *ACTN4* groups. It was considered that the number of patients in the subgroup of *ACTN4* was too small to statistically prove the clinical benefit of chemotherapy alone in the subgroup with CNI of *ACTN4*.

In conclusion, we showed that the copy number of *ACTN4* is not only a prognostic biomarker, but also a candidate predictive biomarker for the decision regarding effective treatment strategy. Although this was a retrospective study, it suggested that patients without gene amplification of *ACTN4* should undergo CRT. Although it was concluded that *ACTN4* is a biomarker of potential metastasis, this does not necessarily contraindicate a potential function for *ACTN4* copy number as a predictive biomarker for CRT of LAPC. More detailed analyses, including a prospective study, should be carried out to prove this possibility.

ACKNOWLEDGEMENTS

This work was supported by a Grant-in Aid for Scientific Research (B) and a Challenging Exploratory Research from the Ministry of Education, Culture, Sports, Science and Technology (METX) of Japan (to KH) and the National Cancer Center Research and Development Fund (23-A-38, and 23-A-11; to KH).

CONFLICT OF INTEREST

The authors declare no conflict of interest.

REFERENCES

Berger AC, Garcia Jr. M, Hoffman JP, Regine WF, Abrams RA, Safran H, Konski A, Benson 3rd AB, MacDonald J, Willett CG (2008) Postresection CA 19-9 predicts overall survival in patients with pancreatic cancer treated with adjuvant chemoradiation: a prospective validation by RTOG 9704. *J Clin Oncol* **26**(36): 5918–5922.

Chauffert B, Mornex F, Bonnetain F, Rougier P, Mariette C, Bouche O, Bosset JF, Aparicio T, Mineur L, Azzedine A, Hammel P, Butel J, Stremsdoerfer N, Maingon P, Bedenne L (2008) Phase III trial comparing intensive induction chemoradiotherapy (60Gy, infusional 5-FU and intermittent cisplatin) followed by maintenance gemcitabine with gemcitabine alone for locally advanced unresectable pancreatic cancer. Definitive results of the 2000-01 FFCD/SFRO study. *Ann Oncol* **19**(9): 1592–1599.

Colucci G, Giuliani F, Gebbia V, Biglietto M, Rabitti P, Uomo G, Cigolari S, Testa A, Maiello E, Lopez M (2002) Gemcitabine alone or with cisplatin for the treatment of patients with locally advanced and/or metastatic pancreatic carcinoma: a prospective, randomized phase III study of the Gruppo Oncologia dell'Italia Meridionale. *Cancer* **94**(4): 902–910.

Crane CH, Varadhachary GR, Yordy JS, Staerkel GA, Javle MM, Safran H, Haque W, Hobbs BD, Krishnan S, Fleming JB, Das P, Lee JE, Abbruzzese JL, Wolff RA (2011) Phase II trial of cetuximab, gemcitabine, and oxaliplatin followed by chemoradiation with cetuximab for locally advanced (T4) pancreatic adenocarcinoma: correlation of Smad4(Dpc4) immunostaining with pattern of disease progression. *J Clin Oncol* **29**(22): 3037–3043.

Hayashida Y, Honda K, Idogawa M, Ino Y, Ono M, Tsuchida A, Aoki T, Hirohashi S, Yamada T (2005) E-cadherin regulates the association between beta-catenin and actinin-4. *Cancer Res* **65**(19): 8836–8845.

Honda K, Okusaka T, Felix K, Nakamori S, Sata N, Nagai H, Ioka T, Tsuchida A, Shimahara T, Shimahara M, Yasunami Y, Kuwabara H, Sakuma T, Otsuka Y, Ota N, Shitashige M, Kosuge T, Buchler MW, Yamada T (2012) Altered plasma apolipoprotein modifications in patients with pancreatic cancer: protein characterization and multi-institutional validation. *PLoS One* **7**(10): e46908.

Honda K, Yamada T, Endo R, Ino Y, Gotoh M, Tsuda H, Yamada Y, Chiba H, Hirohashi S (1998) Actinin-4, a novel actin-bundling protein associated with cell motility and cancer invasion. *J Cell Biol* **140**(6): 1383–1393.

Honda K, Yamada T, Hayashida Y, Idogawa M, Sato S, Hasegawa F, Ino Y, Ono M, Hirohashi S (2005) Actinin-4 increases cell motility and promotes lymph node metastasis of colorectal cancer. *Gastroenterology* **128**(1): 51–62.

Huguet F, Andre T, Hammel P, Artru P, Balosso J, Selle F, Deniaud-Alexandre E, Ruszniewski P, Touboul E, Labianca R, de Gramont A, Louvet C (2007) Impact of chemoradiotherapy after disease control with chemotherapy in locally advanced pancreatic adenocarcinoma in GERCOR phase II and III studies. *J Clin Oncol* **25**(3): 326–331.

Ikeda M, Okusaka T, Ito Y, Ueno H, Morizane C, Furuse J, Ishii H, Kawashima M, Kagami Y, Ikeda H (2007) A phase I trial of S-1 with concurrent radiotherapy for locally advanced pancreatic cancer. *Br J Cancer* **96**(11): 1650–1655.

Johung K, Saif MW, Chang BW (2012) Treatment of locally advanced pancreatic cancer: the role of radiation therapy. *Int J Radiat Oncol Biol Phys* **82**(2): 508–518.

Katz MH, Marsh R, Herman JM, Shi Q, Collison E, Venook AP, Kindler HL, Alberts SR, Philip P, Lowy AM, Pisters PW, Posner MC, Berlin JD, Ahmad SA (2013) Borderline resectable pancreatic cancer: need for standardization and methods for optimal clinical trial design. *Ann Surg Oncol* **20**(8): 2787–2795.

Kikuchi S, Honda K, Handa Y, Kato H, Yamashita K, Umaki T, Shitashige M, Ono M, Tsuchida A, Aoki T, Hirohashi S, Yamada T (2007) Serum albumin-associated peptides of patients with uterine endometrial cancer. *Cancer Sci* **98**(6): 822–829.

Kikuchi S, Honda K, Tsuda H, Hiraoka N, Imoto I, Kosuge T, Umaki T, Onozato K, Shitashige M, Yamaguchi U, Ono M, Tsuchida A, Aoki T, Inazawa J, Hirohashi S, Yamada T (2008) Expression and gene amplification of actinin-4 in invasive ductal carcinoma of the pancreas. *Clin Cancer Res* **14**(17): 5348–5356.

Loehrer Sr. PJ, Feng Y, Cardenes H, Wagner L, Brell JM, Cella D, Flynn P, Ramanathan RK, Crane CH, Alberts SR, Benson 3rd AB (2011) Gemcitabine alone versus gemcitabine plus radiotherapy in patients with locally advanced pancreatic cancer: an Eastern Cooperative Oncology Group trial. *J Clin Oncol* **29**(31): 4105–4112.

Mayahara H, Ito Y, Morizane C, Ueno H, Okusaka T, Kondo S, Murakami N, Morota M, Sumi M, Itami J (2012) Salvage chemoradiotherapy after primary chemotherapy for locally advanced pancreatic cancer: a single-institution retrospective analysis. *BMC Cancer* **12**: 609.

Mian OY, Ram AN, Tuli R, Herman JM (2014) Management options in locally advanced pancreatic cancer. *Curr Oncol Rep* **16**(6): 388.

Miyanaga A, Honda K, Tsuta K, Masuda M, Yamaguchi U, Fujii G, Miyamoto A, Shinagawa S, Miura N, Tsuda H, Sakuma T, Asamura H, Gemma A, Yamada T (2013) Diagnostic and prognostic significance of the alternatively spliced ACTN4 variant in high-grade neuroendocrine pulmonary tumours. *Ann Oncol* **24**(1): 84–90.

Moore MJ, Goldstein D, Hamm J, Figer A, Hecht JR, Gallinger S, Au HJ, Murawa P, Walde D, Wolff RA, Campos D, Lim R, Ding K, Clark G, Voskoglou-Nomikos T, Ptasynski M, Parulekar W. National Cancer Institute of Canada Clinical Trials G (2007) Erlotinib plus gemcitabine compared with gemcitabine alone in patients with advanced pancreatic cancer: a phase III trial of the National Cancer Institute of Canada Clinical Trials Group. *J Clin Oncol* **25**(15): 1960–1966.

Noro R, Honda K, Tsuta K, Ishii G, Maeshima AM, Miura N, Furuta K, Shibata T, Tsuda H, Ochiai A, Sakuma T, Nishijima N, Gemma A, Asamura H, Nagai K, Yamada T (2013) Distinct outcome of stage I lung adenocarcinoma with ACTN4 cell motility gene amplification. *Ann Oncol* **24**(10): 2594–2600.

Otey CA, Carpen O (2004) Alpha-actinin revisited: a fresh look at an old player. *Cell Motil Cytoskeleton* **58**(2): 104–111.

Pawlik TM, Laheru D, Hruban RH, Coleman J, Wolfgang CL, Campbell K, Ali S, Fishman EK, Schulick RD, Herman JM. Johns Hopkins Multidisciplinary Pancreas Clinic T (2008) Evaluating the impact of a single-day multidisciplinary clinic on the management of pancreatic cancer. *Ann Surg Oncol* **15**(8): 2081–2088.

Savir G, Huber KE, Saif MW (2013) Locally advanced pancreatic cancer. Looking beyond traditional chemotherapy and radiation. *JOP* **14**(4): 337–339.

Watabe Y, Mori T, Yoshimoto S, Nomura T, Shibahara T, Yamada T, Honda K (2014) Copy number increase of ACTN4 is a prognostic indicator in salivary gland carcinoma. *Cancer Med* **3**(3): 613–622.

Welsch T, Keleg S, Bergmann F, Bauer S, Hinz U, Schmidt J (2009) Actinin-4 expression in primary and metastasized pancreatic ductal adenocarcinoma. *Pancreas* **38**(8): 968–976.

Yamamoto S, Tsuda H, Honda K, Kita T, Takano M, Tamai S, Inazawa J, Yamada T, Matsubara O (2007) Actinin-4 expression in ovarian cancer: a novel prognostic indicator independent of clinical stage and histological type. *Mod Pathol* **20**(12): 1278–1285.

Yamamoto S, Tsuda H, Honda K, Onozato K, Takano M, Tamai S, Imoto I, Inazawa J, Yamada T, Matsubara O (2009) Actinin-4 gene amplification in ovarian cancer: a candidate oncogene associated with poor patient prognosis and tumor chemoresistance. *Mod Pathol* **22**(4): 499–507.

Yamamoto S, Tsuda H, Honda K, Takano M, Tamai S, Imoto I, Inazawa J, Yamada T, Matsubara O (2012) ACTN4 gene amplification and actinin-4 protein overexpression drive tumour development and histological progression in a high-grade subset of ovarian clear-cell adenocarcinomas. *Histopathology* **60**(7): 1073–1083.

Yang GY, Malik NK, Chandrasekhar R, Ma WW, Flaherty L, Iyer R, Kuvshinoff B, Gibbs J, Wilding G, Warren G, May KS (2013) Change in CA 19-9 levels after chemoradiotherapy predicts survival in patients with locally advanced unresectable pancreatic cancer. *J Gastrointest Oncol* **4**(4): 361–369.

Supplementary Information accompanies this paper on British Journal of Cancer website (http://www.nature.com/bjc)

The Laryngoscope

Expression of EpCAM and Prognosis in Early-Stage Glottic Cancer Treated by Radiotherapy

Naoya Murakami, MD, PhD; Taisuke Mori, DMD, PhD; Seiichi Yoshimoto, MD, PhD; Yoshinori Ito, MD; Kazuma Kobayashi, MD; Harada Ken, MD; Mayuka Kitaguchi, MD; Shuhei Sekii, MD; Kana Takahashi, MD; Kotaro Yoshio, MD, PhD; Koji Inaba, MD; Madoka Morota, MD, PhD; Minako Sumi, MD, PhD; Jun Itami, MD, PhD

Objectives/Hypothesis: Treatment of head and neck squamous cell carcinoma (HNSCC) often requires radiotherapy, but relapse can occur. There is, therefore, an urgent need for the identification of a predictive novel biomarker for radiosensitivity. The epithelial cell adhesion molecule (EpCAM) has been shown to promote the transformation of malignant tumors, and EpCAM may have prognostic significance, but it is not known if EpCAM determines prognosis, especially with respect to radiotherapy. Therefore, we determined the incidence of the expression of EpCAM in HNSCC and analyzed the prognostic value in patients with early-stage glottic cancer treated with radiotherapy.

Study Design: Retrospective analysis.

Methods: All patients with HNSCCs examined in our hospital between January 2012 and February 2013 were analyzed prospectively for the expression of EpCAM. T1–2N0 glottic cancer patients who were primarily treated by radiation therapy between 1995 and 2008 were retrospectively investigated. Patients with or without local recurrence after radical radiation therapy were extracted. The relationship between local recurrence and histopathologic EpCAM expression was compared within these two groups.

Results: One hundred eighteen patients with HNSCCs from the nasopharynx, oropharynx, hypopharynx, larynx, oral cavity, paranasal cavity, unknown primary, and other sites were analyzed. Positive expression of EpCAM was noted in the oropharynx, hypopharynx, and larynx (72%, 90%, and 58%, respectively). Seventeen and 22 patients with or without local recurrence were extracted, respectively. There was no difference between two groups, with the exception of EpCAM expression.

Conclusions: The expression of EpCAM in HNSCC was investigated. Patients with strong EpCAM expression were associated with local recurrence after primary radiation therapy.

Key Words: Head and neck squamous cell carcinoma, EpCAM, BerEP4, early-stage glottic cancer, radiation therapy.

Level of Evidence: NA

***Laryngoscope*, 124:E431–E436, 2014**

INTRODUCTION

Radiation therapy with or without chemotherapy is established as a curative modality for head and neck squamous cell carcinoma (HNSCC)[1–3]; however, tumor resistance to radiation therapy often occurs, especially for advanced-stage tumors. Therefore, the search for biomarkers with prognostic relevance has been studied in radiation therapy of HNSCC over the past several decades. Identification of such biomarkers enables the selection of patients for more suitable treatment modalities based on specific tumor biology. Epidermal growth factor receptor, p53, and p16 (a surrogate marker for human papillomavirus [HPV] infection) are well-known prognostic factors with respect to radiation therapy for HNSCCs.[4–9] It has been demonstrated that HPV-positive HNSCCs are very radiosensitive; however, HPV-positive HNSCCs arise predominantly from the oropharynx.[7] Therefore, another reliable predictive factor for the outcome of radiation therapy for HNSCCs is needed.

Cell adhesions are an essential process required for the appropriate functioning of multicellular organisms. It has been shown that cell adhesion molecules play multiple roles, including cell-cell and cell-matrix interactions, cell migration, cell cycle, signaling, and morphogenesis, during tissue development and regeneration.[10] Epithelial cell adhesion molecule (EpCAM) is a 40 kDA epithelial type I trans-membrane glycoprotein expressed on most normal human epithelial tissues and human

From the Department of Radiation Oncology (N.M., Y.I., K.K., H.K., M.K., S.S., K.T., K.Y., K.I., M.M., M.S., J.I.), Department of Clinical Laboratory and Pathology (T.M.), and the Department of Head and Neck Surgery (S.Y.), National Cancer Center Hospital, Tokyo, Japan

Editor's Note: This Manuscript was accepted for publication June 25, 2014.

Presented as an e-poster at the ESTRO 33 Meeting, Vienna, Austria, April 4–8, 2014.

This study was partially supported by the Cancer Research Development Fund 23A-13. The funding body was the National Cancer Center.

The authors have no other funding, financial relationships, or conflicts of interest to disclose.

Send correspondence to Naoya Murakami, MD, Department of Radiation Oncology, National Cancer Center Hospital, 5-1-1 Tsukiji, Chuo-ku, Tokyo 104-0045, Japan; e-mail: namuraka@ncc.go.jp; and Taisuke Mori, DMD, Department of Clinical Laboratory and Pathology, National Cancer Center Hospital, 5-1-1 Tsukiji, Chuo-ku, Tokyo 104-0045, Japan; e-mail: tamori@ncc.go.jp

DOI: 10.1002/lary.24839

carcinomas.[11] EpCAM is considered as a marker for human epithelial tissues and malignant epithelial tumors. Accumulating evidence has shown that EpCAM is frequently expressed on human epithelial malignant tumors (predominantly on adenocarcinomas), and is stably expressed or even upregulated during the progression of disease.[12,13] It has also been demonstrated that EpCAM could be a prognostic marker for breast cancer,[14] esophageal cancer,[15] and uterine cervical cancer[16]; however, few studies exist regarding the relationship between EpCAM expression and radiosensitivity.[16]

We prospectively evaluated EpCAM expression on consecutive tissue specimens from January 2012 (study I) to determine the incidence of EpCAM positive tumors in HNSCCs. Because the follow-up period was limited, it was difficult to assess the prognostic significance of EpCAM for radiation therapy. Therefore, to determine the relationship between the expression of EpCAM and response of radiation therapy, we focused on early-stage glottic cancer, which is usually treated by a uniformly fashioned radiation therapy technique (study II).

MATERIALS AND METHODS

Cases

Study I. After approval of our institutional review board, we prospectively collected formalin-fixed, paraffin-embedded specimens from all of the HNSCC patients. The specimens included biopsies and surgically removed specimens. The study period was January 2012 to February 2013, and 118 HNSCC cases were included in this study. The median age of the 118 patients (95 males and 23 females) was 67 years (mean, 65.9 ± 12.6 years). All specimens were reviewed in our institution, and the histological tumor types were classified according to the World Health Organization (WHO) criteria.[17]

Immunohistochemical Analysis

Sections (4-μm thick) from the representative block of each tumor were routinely deparaffinized. The sections were subjected to hematoxylin-eosin and immunohistochemical staining. Immunohistochemical staining was performed with the following primary antibodies: EpCAM (1:200, ab7504, Ber-EP4; Abcam, Cambridge, MA)[18]; p53 (1:400, DO-7, Dako, Carpinteria, CA); and p16 (1:50, p16ink4a, G175–405; BD Biosciences, San Jose, CA). Each section was exposed to 0.3% hydrogen peroxide for 15 minutes to block endogenous peroxidase activity. For staining, we used an automated stainer (Dako) according to the protocol of the manufacturer. ChemMate EnVision (Dako) methods were used for detection. Appropriate positive and negative controls were used for each antibody. BerEP4 positivity was defined as follows: minus (−), no expression; one plus (+), weak-to-moderate expression; and two plus (++), intense expression. The typical staining patterns of BerEP4 are shown in Figure 1. Additionally, p53 and p16, well-known prognostic factors for HNSCCs, were also analyzed. Briefly, strong expression of nuclear p53 (accumulation) or no expression (missense of exon 5–9 of p53, where most known abnormalities occur) was considered to represent a p53 gene mutation[19,20]; otherwise, tumors were considered not to have a p53 mutation. For p16, only tumors with expression in the cytoplasm and nucleus were considered to be HPV infected; otherwise, tumors were considered to be noninfected with HPV. The sensitivity and the specificity of p16 immunohistochemistry were 94% and 82%, respectively, based on our past experience, which is nearly identical to a previous report.[21]

Study II. T1–2N0 glottic cancer patients who were primarily treated by radiation therapy between April 1995 and December 2008 were retrospectively investigated. Tumor T stage was re-evaluated according to the 7th edition of the American Joint Committee on Cancer/International Union Against Cancer.[22] Whether or not tumor was exophytic and had direct invasion to the anterior commissure was also assessed. Patients with or without a local recurrence after radical external beam radiation therapy (EBRT) were extracted. Among patients with a local recurrence, only patients with a local recurrence on the ipsilateral side and the same part of the glottis were included. Patients whose pretreatment pathological examination was performed in different institutions and whose biopsy specimen was too small were excluded from this study because it was difficult to perform another immunohistopathologic examination. Patients without local or regional recurrence were also extracted as a control. These patients had similar T stages, gender, radiation doses, and treatment periods as patients with local recurrences. Patients were treated with a continuous course of EBRT delivered by a ^{60}Co (patients treated before March 1998) or linear accelerator (patients treated after April 1999). All of the patients were treated by opposing fields. It is well known that the control rate of early-stage glottic cancer treated by radiation therapy is affected by radiation energy, fraction size, total dose, and overall time.[23,24] Therefore, information about radiation technique was also collected, and patients were divided into two groups according to the radiation techniques applied. Group 1 was defined as patients who met at least one of the following definitions: treated with $\geq$6 MV without using a bolus; total dose <66 Gy in 2-Gy fractions or 60 Gy in 2.4-Gy fractions for T1 or <70 Gy in 2-Gy fractions or 64.8 Gy in 2.4-Gy fractions for T2; and total treated time >51 days in 2-Gy fractions or 39 days in 2.4-Gy fractions for T1 or >53 days in 2-Gy fractions or 43 days in 2.4-Gy fractions for T2. The remaining patients were classified in group 2. Expression of BerEP4, p53, and p16 was assessed based on a biopsy specimen obtained before primary radiation therapy. The relationship between clinical results and demographic or therapeutic characteristics were compared between patients with or without a local recurrence. The Student unpaired t test was used to compare the continuous variables, and Pearson χ^2 test was used to compare categorical variables. A P value <.05 was considered statistically significant. All statistical analyses were performed using SPSS Statistics (version 18.0; SPSS, Inc., Chicago, IL). This retrospective study was also approved by the institutional review board of our hospital according to the ethical standards laid down in the Declaration of Helsinki.

RESULTS

Study I

Table I shows the distribution of expression of BerEP4, p53, and p16 according to tumor sites for HNSCCs. There were 52 HNSCCs from the oral cavity, 28 from the oropharynx, 20 from the hypopharynx, 13 from the larynx, and five from miscellaneous sites. The BerEP4-positive rate of HNSCCs from the oropharynx, hypopharynx, and larynx were higher than from the oral cavity. The overall BerEP4-positive rate, which combined + with ++ and the rate of BerEP4 ++ tumors in HNSCCs from the hypopharynx, was the highest among all the other sites. There was no statistical difference between the p53 mutation status among different

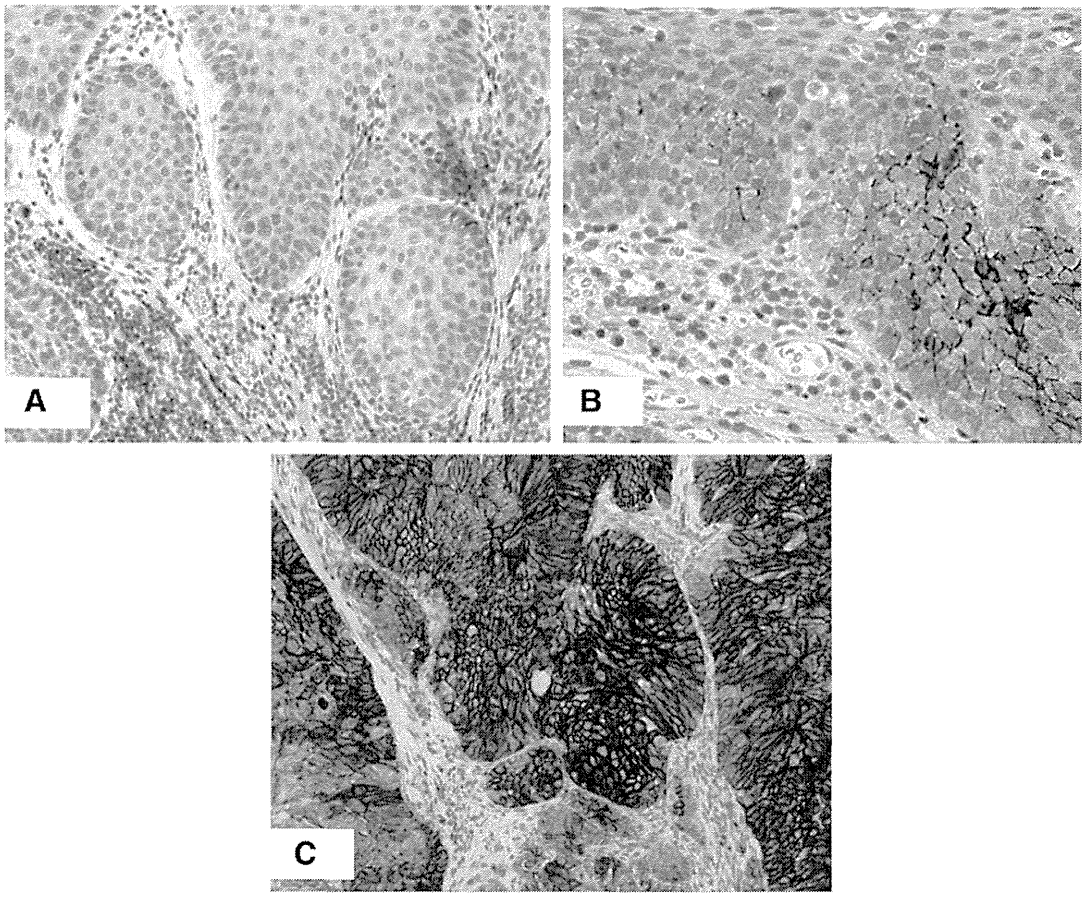

Fig. 1. The typical staining patterns of BerEP4 are shown. The positivity of BerEP4 was defined as follows: (A) minus (−), no expression; (B) one plus (+), weak-to-moderate expression, (C) two plus (++), intense expression. [Color figure can be viewed in the online issue, which is available at www.laryngoscope.com.].

primary sites. As is well known from other reports, the p16 immunohistochemical/HPV-infected pattern was the most frequently seen in HNSCCs from the oropharynx.

Study II

Between April 1995 and December 2008, 241 patients were identified who were treated by primary radiation therapy for T1–2N0 early-stage glottic cancer. Thirty-six patients had tumor recurrences; 32 patients suffered from the local recurrences. Three patients were excluded because they had a recurrent tumor in a different part of the glottis. Of the remaining 29 patients, only 17 had a tumor specimen large enough to undergo additional immunohistopathologic examinations stored in the hospital, thus these 17 patients comprise the case cohort. For controls, 22 patients were selected from

TABLE I.
Expression of BerEP4, p53, and p16 According to Tumor Site for Head and Neck Squamous Cell Carcinoma.

		BerEP4					p53				p16			
	No.	N/A*	(−)	(+)	(++)	*P*	N/A*	Without Mutation	With Mutation	*P*	N/A*	HPV Uninfected Pattern	HPV Infected Pattern	*P*
Oral cavity	52	2	28	18	4	.03†	0	13	39	.092	16	34	2	.005†
Oropharynx	28	0	8	14	6		0	8	20		1	18	9	
Hypopharynx	20	0	2	8	10		0	1	19		7	12	1	
Larynx	13	1	4	5	3		1	2	9		3	9	0	
Others	5	0	1	4	0		0	2	3		2	1	2	

*N/A = not available. Because of the small amount of biopsy specimens, it was impossible to perform another immunohistopathological examination.
†A *P* value <.05 was considered statistically significant.
HPV = human papillomavirus.